

Small-scale structure at high redshift: observability and effects on reionization

Ilian T Iliev

CITA, Toronto

KITP Santa Barbara, Feb. 2005

Collaborators:

- Paul Shapiro, Kyungjin Ahn, Marcelo Alvarez (UT Austin)
- Evan Scannapieco (KITP, UCSB)
- Ue-Li Pen, Dick Bond, Hugh Merz (CITA)
- Garrelt Mellema (ASTRON, Netherlands)
- Alejandro Raga (UNAM, Mexico)
- Hugo Martel (Laval, Canada)
- Andrea Ferrara (SISSA, Italy)
- Hy Trac (Princeton)

Outline

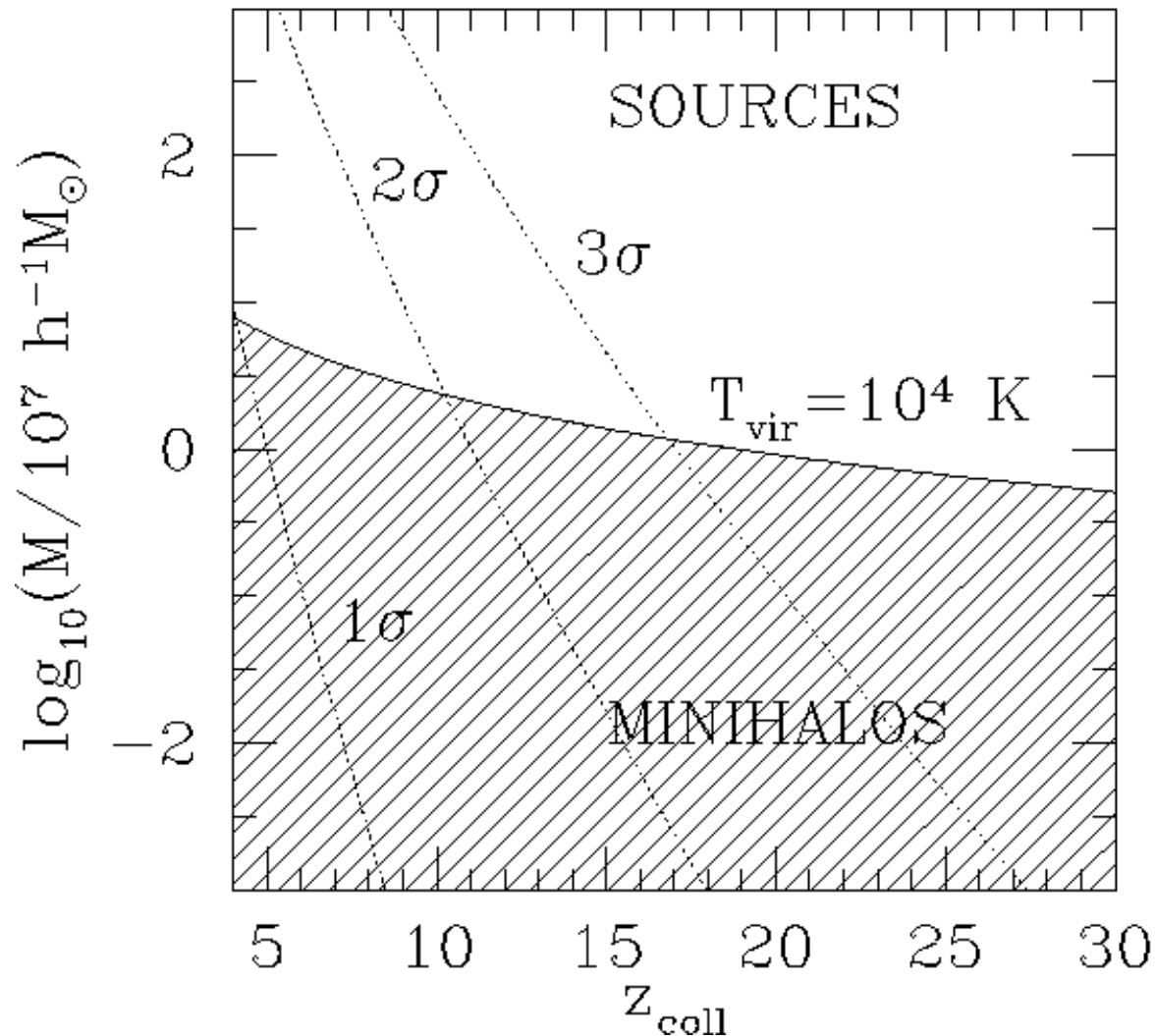
- Structure formation at high- z
- Cosmological I-Fronts
- New radiative transfer code
- Photoevaporation of cosmological minihalos
- Effect of small-scale structure on progress and duration of Reionization
- Observing structures in the Cosmic Dark Ages and Reionization at 21-cm line of H

The Epoch of Reionization

- GP troughs detected in spectra of SDSS quasars at $z > 6 \implies$ IGM H I density high enough to suggest reionization only just ended at $z \sim 6$.
- WMAP detection of CMB polarization fluctuations on large angular scale \implies foreground electron scattering optical depth high enough to suggest IGM mostly ionized by $z > 12$.
- Plausible explanation: reionization began by $z > 15$ but was extended in time, with final “overlap” of ionized zones at $z \sim 6$.
- Can small-scale structure forming at high- z help?

How common were minihalos at high redshift?

Λ CDM, $\Omega_0 = 1 - \lambda_0 = 0.3$, $h = 0.7$



Structure Formation at High- z

(Iliev, Pen, Merz, Trac, Shapiro, and Ahmic in prep.)

We performed very high-resolution N-body simulations of structure formation at high- z using PMFAST code developed at CITA

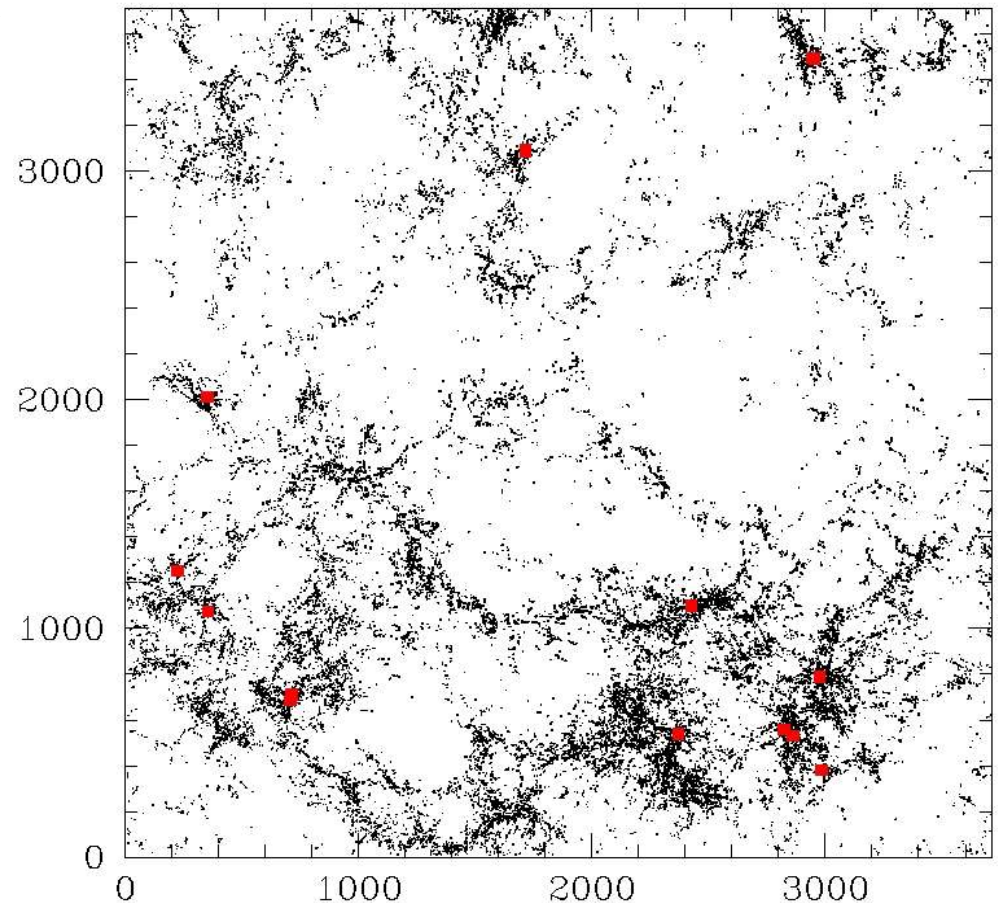
(Merz, Pen & Trac 2004)

Simulation parameters:

- 10/h Mpc box (other box sizes in progress)
- 1856^3 particles (6.4 billion)
- 3712^3 cells
- Identified between 544,000 halos (at $z=17.2$) and 2.3 million halos (at $z=6$) (>100 particles/halo)

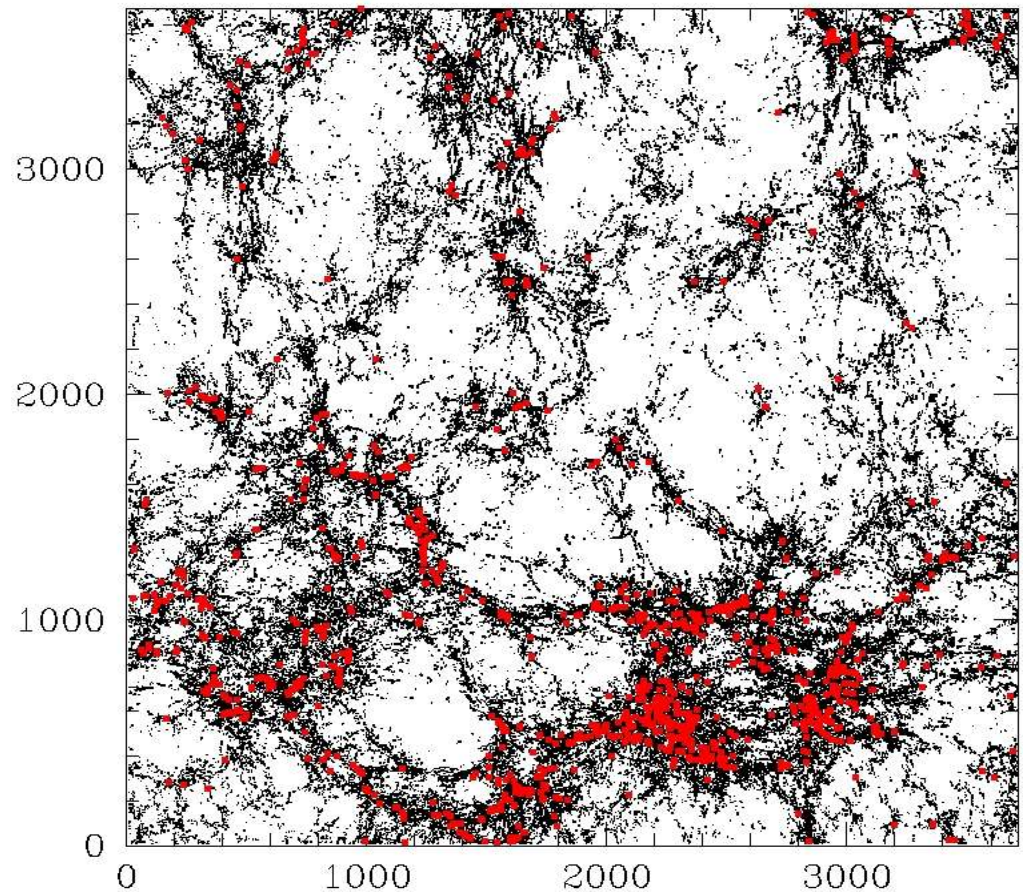
High-resolution N-body simulations

- 1 Mpc slice ($1/14^{\text{th}}$ of the box)
- $z=17.2$
- red=sources (16 halos)
- black=minihalos (32,627 halos)



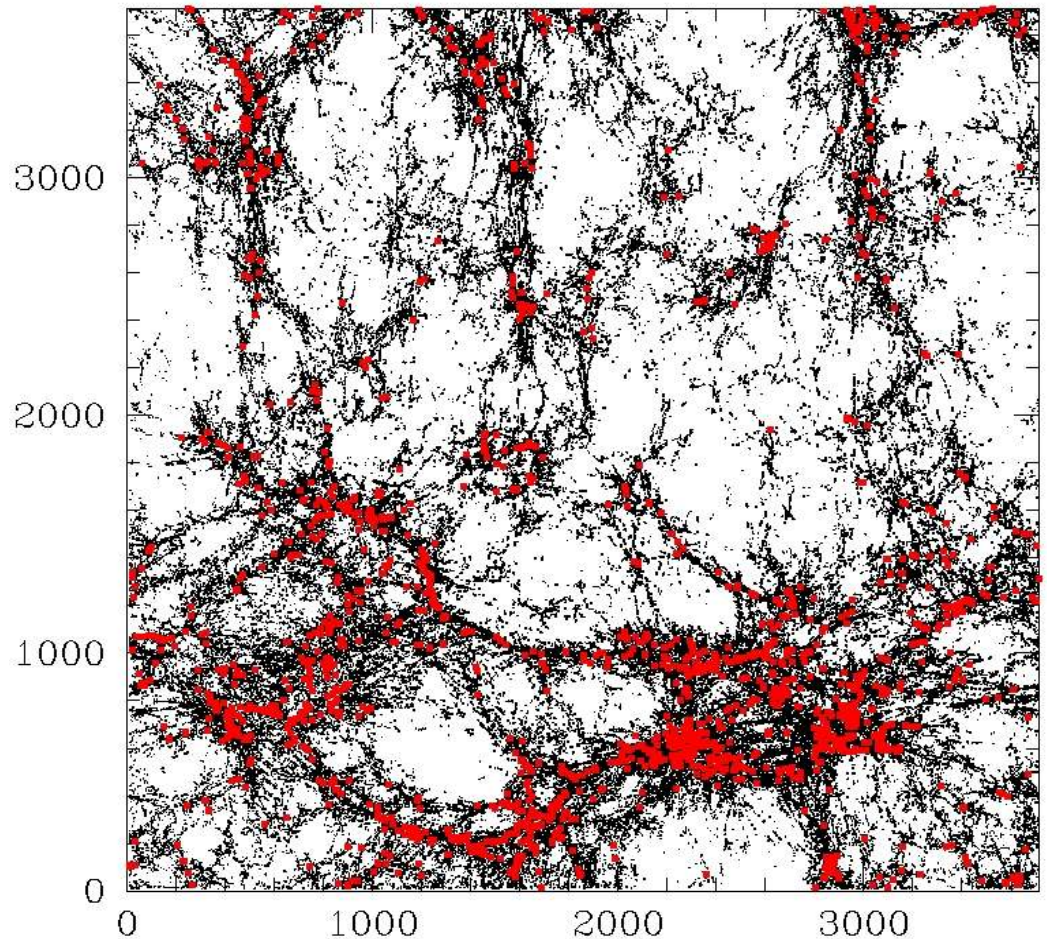
High-resolution N-body simulations

- 1 Mpc slice
- $z=9.42$
- red=sources
(1077 halos)
- black=minihalos
(124,121 halos)

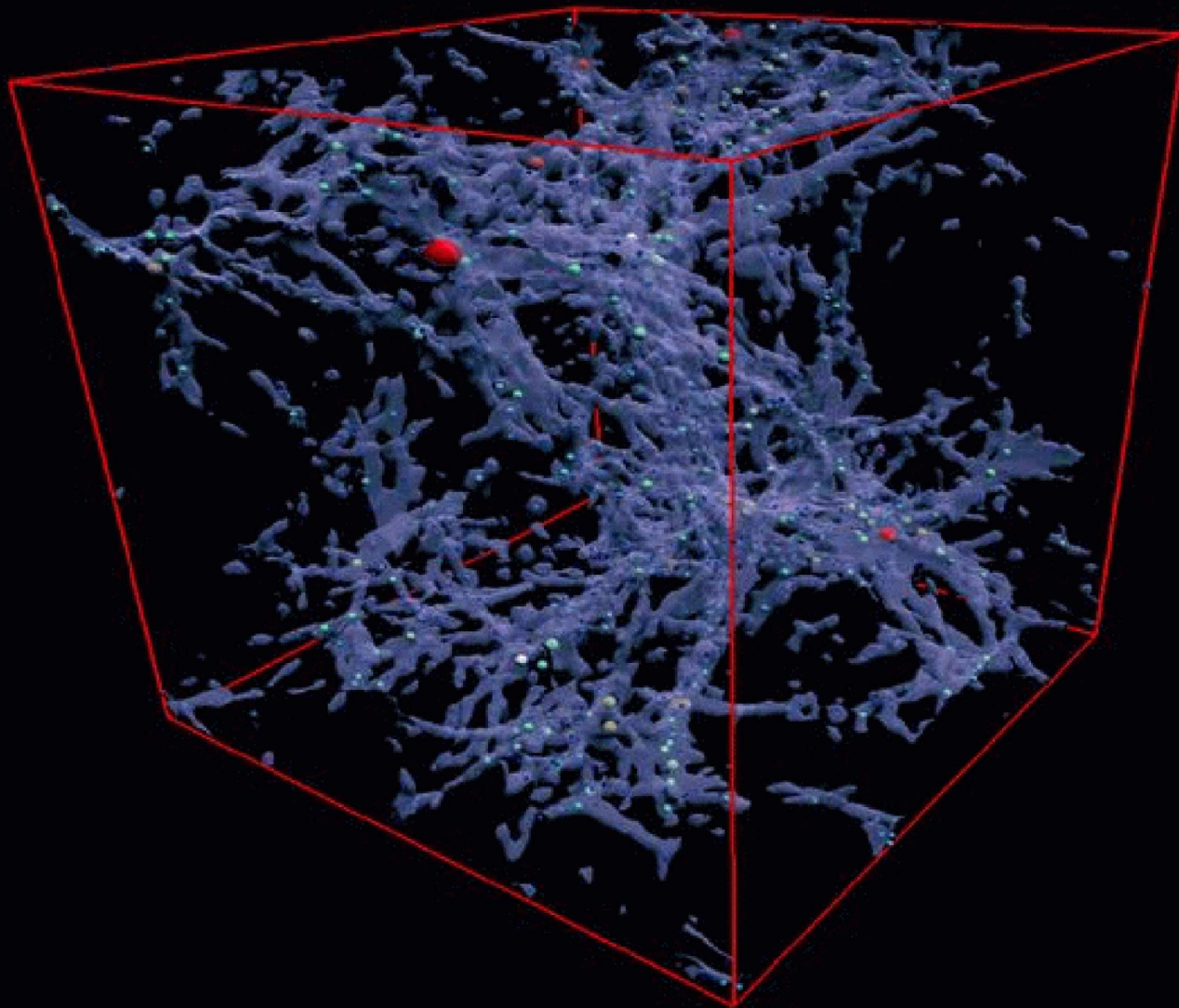


High-resolution N-body simulations

- 1 Mpc slice
- $z=6$
- red=sources
(1672 halos)
- black=minihalos
(142,260 halos)

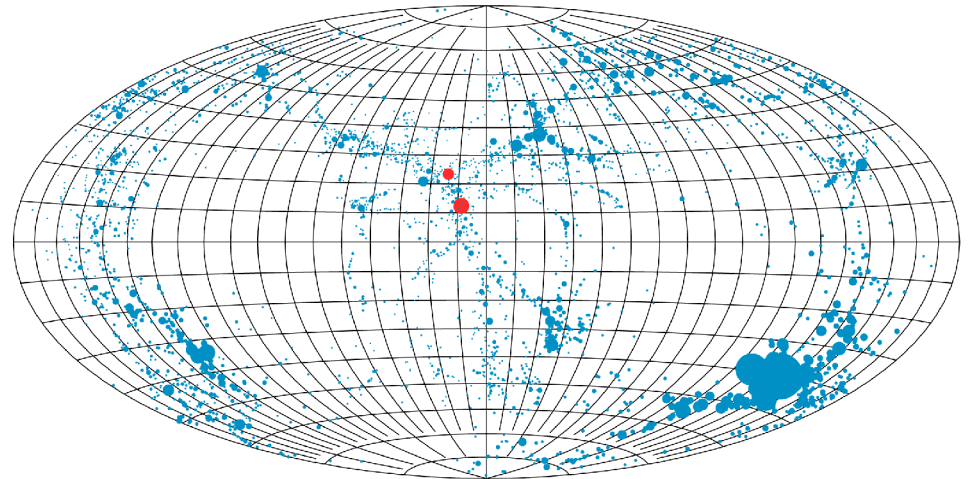


Universe at Redshift $z = 9$

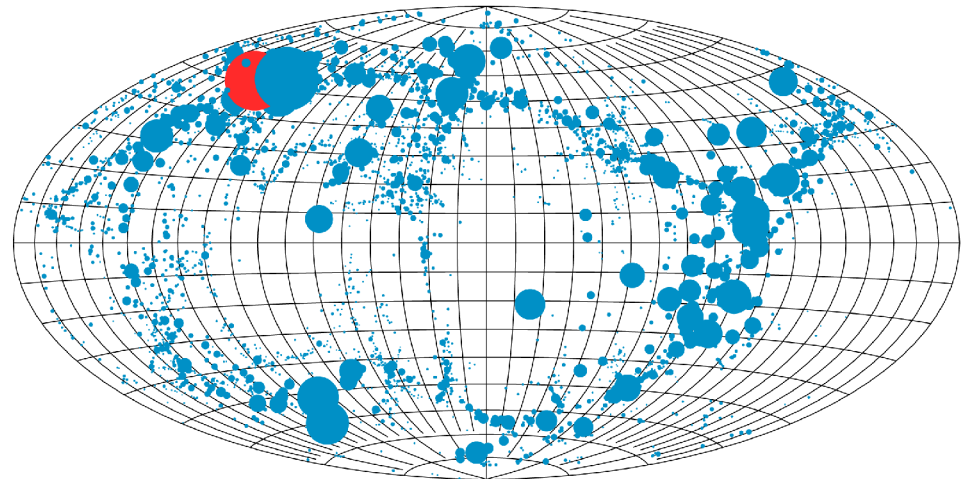


- Minihalos with $T_{\text{vir}} < 10^4 \text{ K}$ were common enough to cover the sky around source halos with $T_{\text{vir}} > 10^4 \text{ K}$ during reionization.

Λ CDM HALOS WITHIN 25 KPC AT $Z = 9$



Sky as seen from a random location
Covering fraction : 10.7%



Sky as seen from a $1.1 \times 10^8 M_{\odot}$ source
Covering fraction : 23.6%

Ionization fronts in the IGM

- The first sources of ionizing radiation to condense out of the dark, neutral, opaque IGM heated and ionized it between $z \sim 30$ and $z \sim 6$.
- Weak, R-type ionization fronts surrounding each source swept outward through the IGM, overtaking other condensations and photoevaporating them.
- High-redshift sources of ionizing photons may have found the sky covered by these minihalos. If so, then minihalos blocked the path of reionization until they photoevaporated.
- This process was largely ignored in previous treatments, but could have had very significant effect on the global reionization, slowing it down and extending it in time.

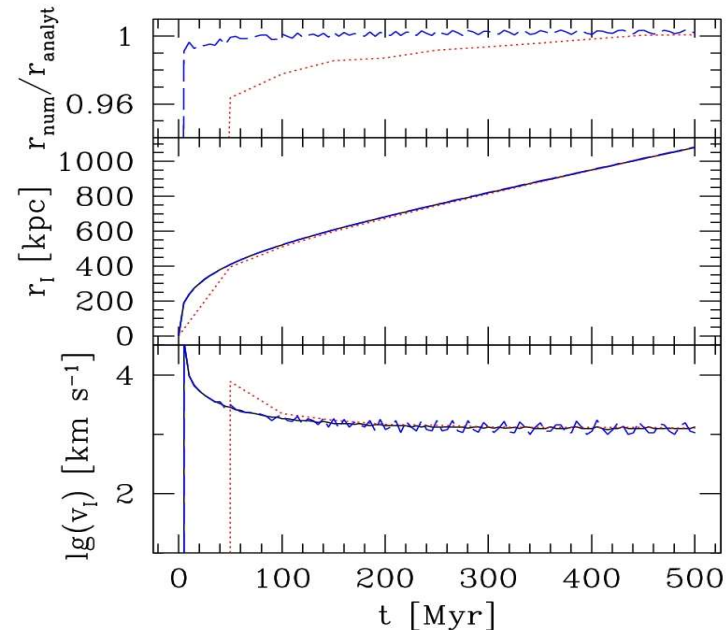
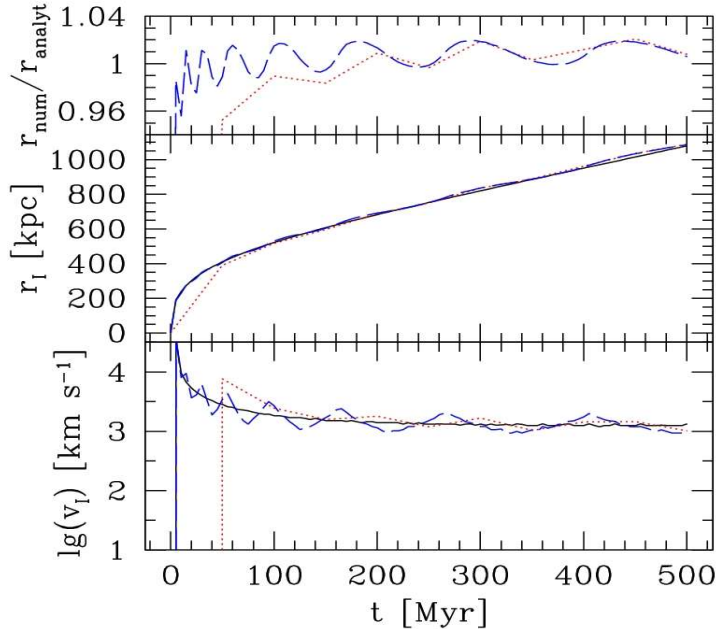
Photon-Conserving Transport of Ionizing Radiation

(Mellema, Iliev, Alvarez & Shapiro, in prep.)

We are developing a new radiative transfer method:

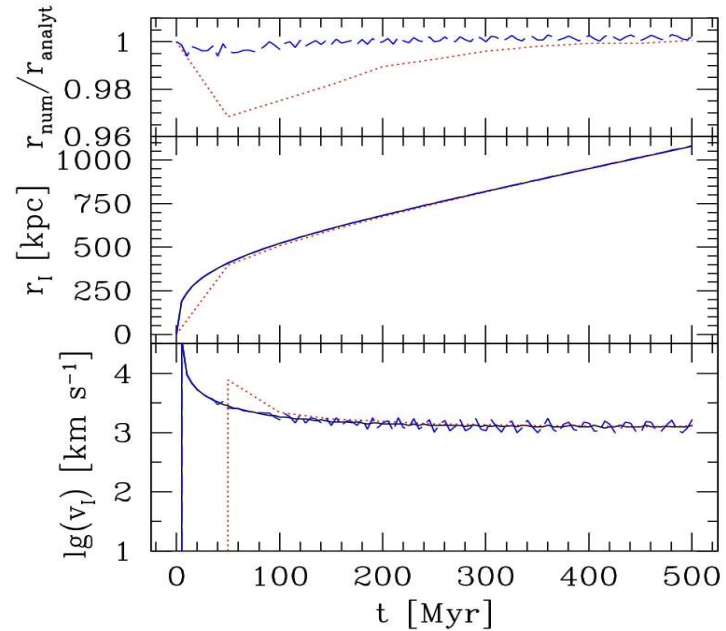
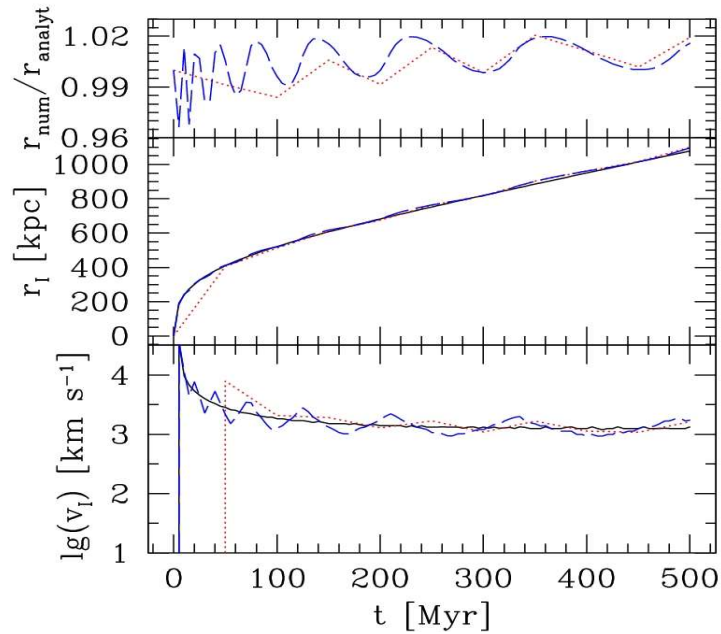
- explicitly photon-conserving. Rates calculated as in Abel, Norman & Madau 00 + averaging in time following non-equilibrium chemistry => much faster, does not require small time-steps to follow fast I-fronts)
- Tested in detail (multiple tests with exact analytical solutions performed, samples on next slides):
 - correctly evolves I-fronts even at very low spatial and time resolutions
 - non-equilibrium chemistry, finds correct temperature
- fast and efficient, easily coupled to hydro and N-body dynamics
- applicable in either cosmological or non-cosmological situations

Tests: I-front propagation in 1-D (sample)



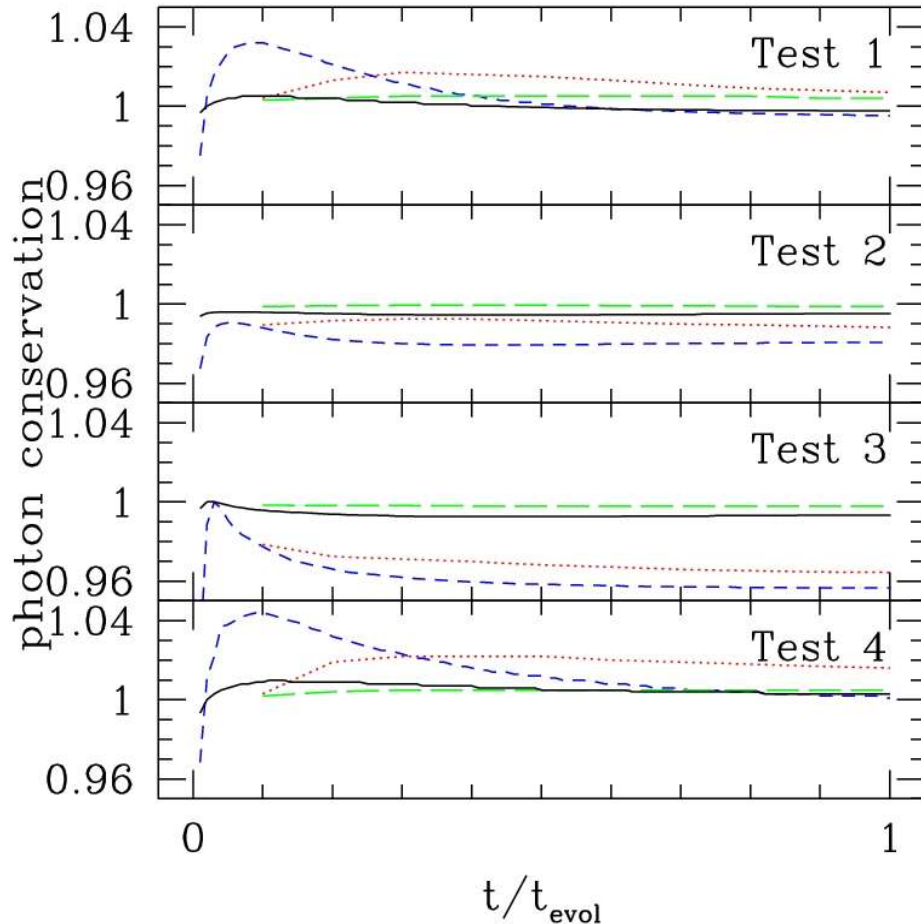
Example: Cosmological I-front propagation, starting at $z=9$, expanding, uniform IGM with mean clumping and fixed temperature (analytical solution exists: Shapiro & Giroux 1987)

Tests: I-front propagation in 3-D (sample)



Same as previous, but in 3D.

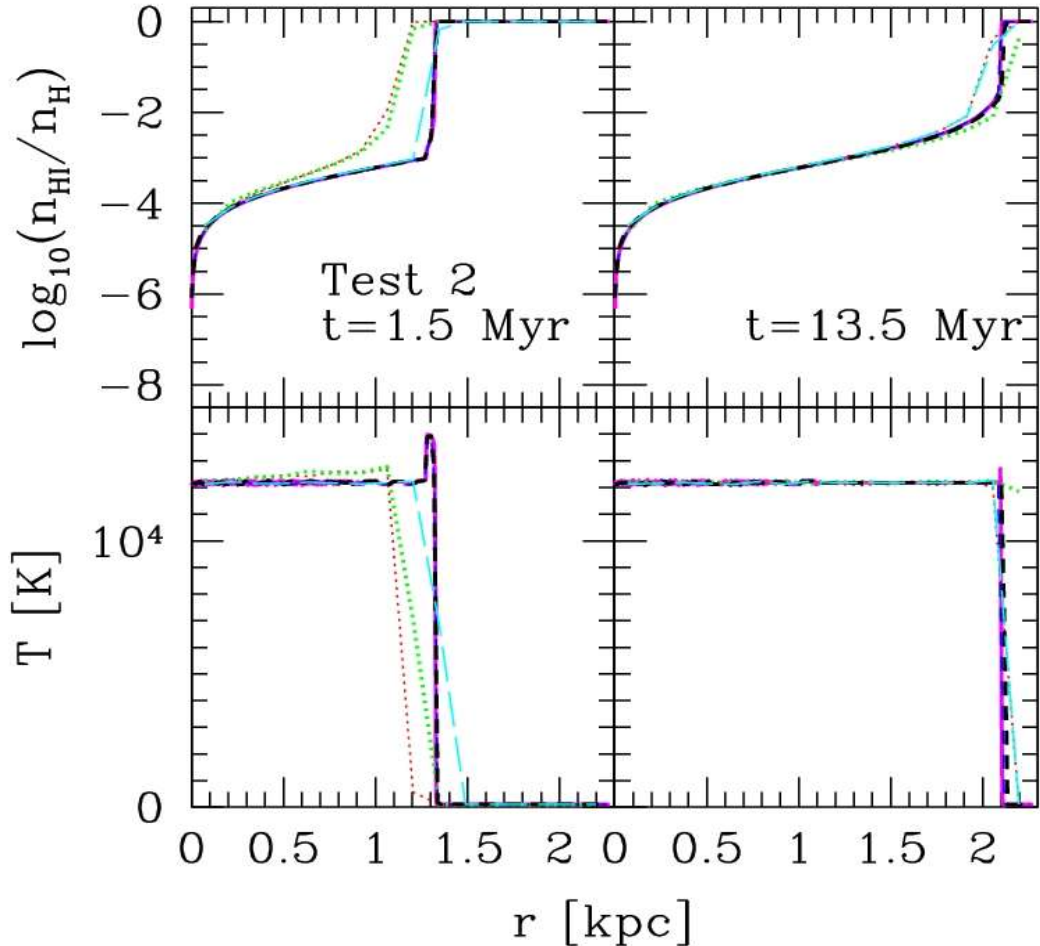
Photon Conservation



Photons are conserved to within few percent at very low resolution and small fraction of 1% at higher resolution

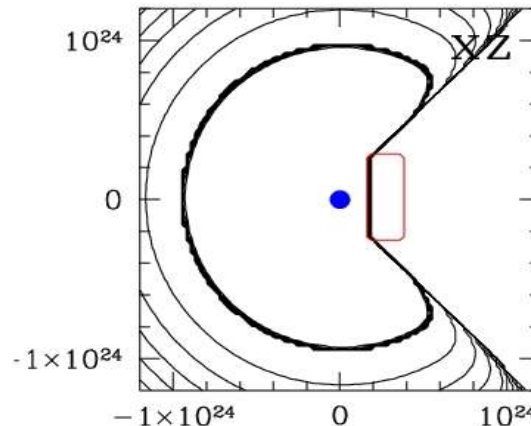
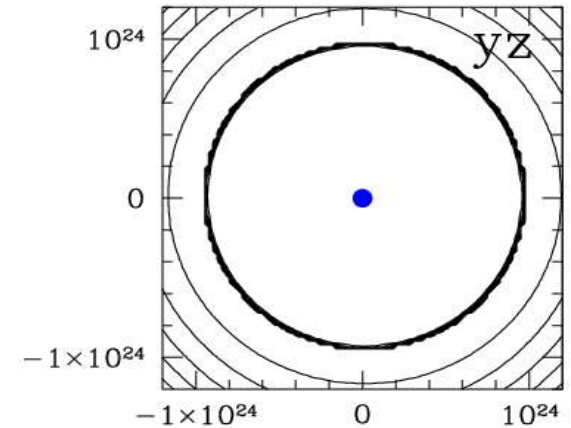
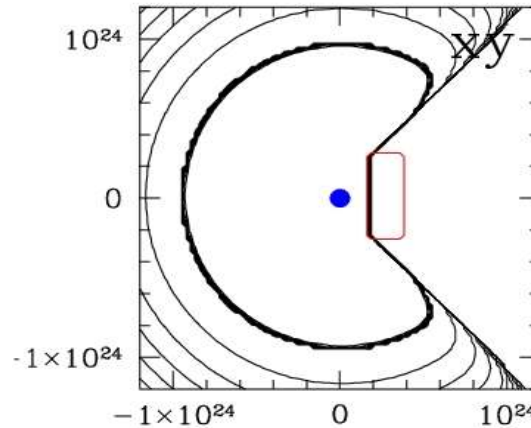
Temperature tests (sample)

- $1/r$ density profile (NFW-like)
- Stromgren sphere reached
- 1-D, 3-D and “analytical” agree, regardless of space/time resolution



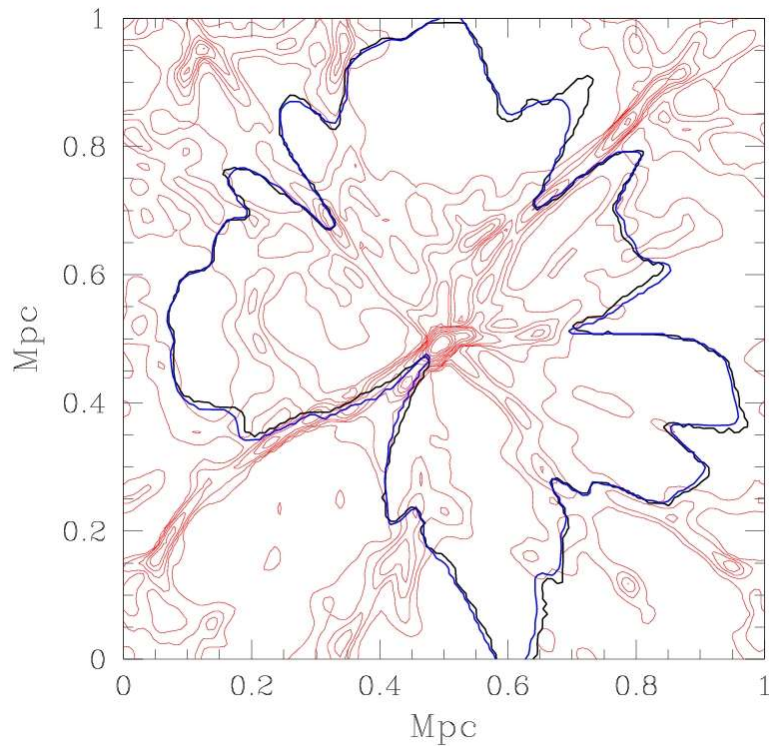
Shadowing Test

- ionizing source (blue)
- dense obstacle (red)
- 256^3 cells
- contours: time-sequence of 50% ionized fraction, every 20 Myr
- I-front is spherical, shadows are at the correct place, there is slight diffusion around the shadow's edges



Shadowing test

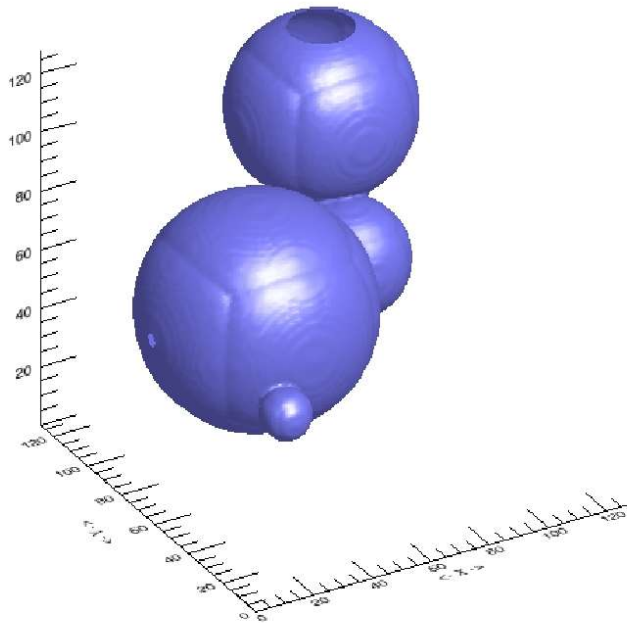
Long- vs. Short-characteristics



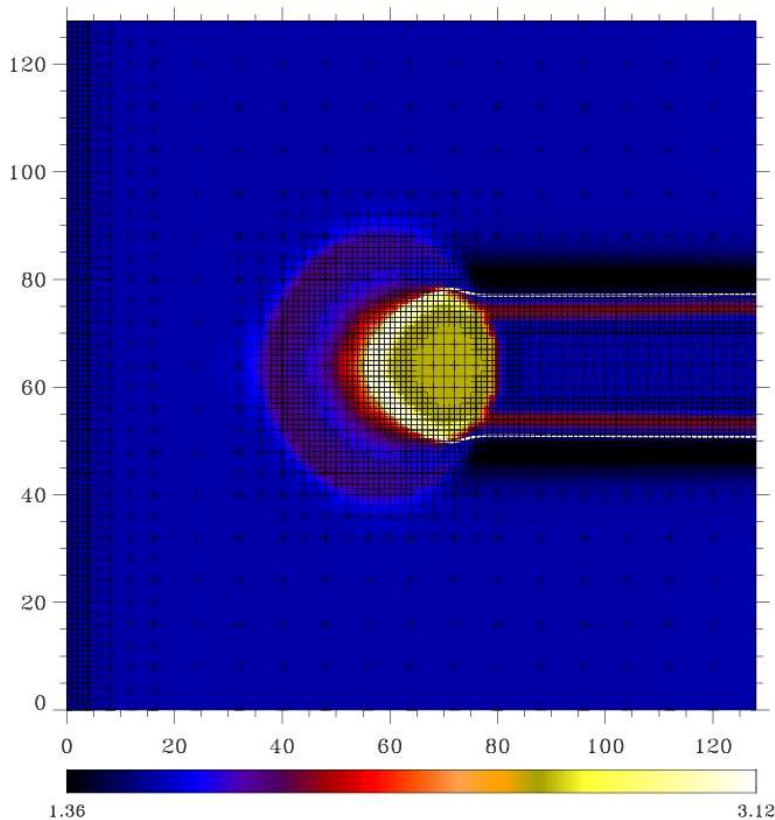
- Long-characteristics is more precise, but slower and more difficult to implement for multiple sources
- Short-characteristics is faster and with appropriately chosen weightings gives same results as LC

Multiple sources

Code correctly follows ionization fronts from multiple sources in the computational volume.



Coupling to AMR Hydrodynamics



Code is now coupled to
adaptive mesh
refinement (AMR)
hydrodynamics code
yguasu.

E.g. plane-parallel
I-front encountering
dense clump and
photoevaporating it

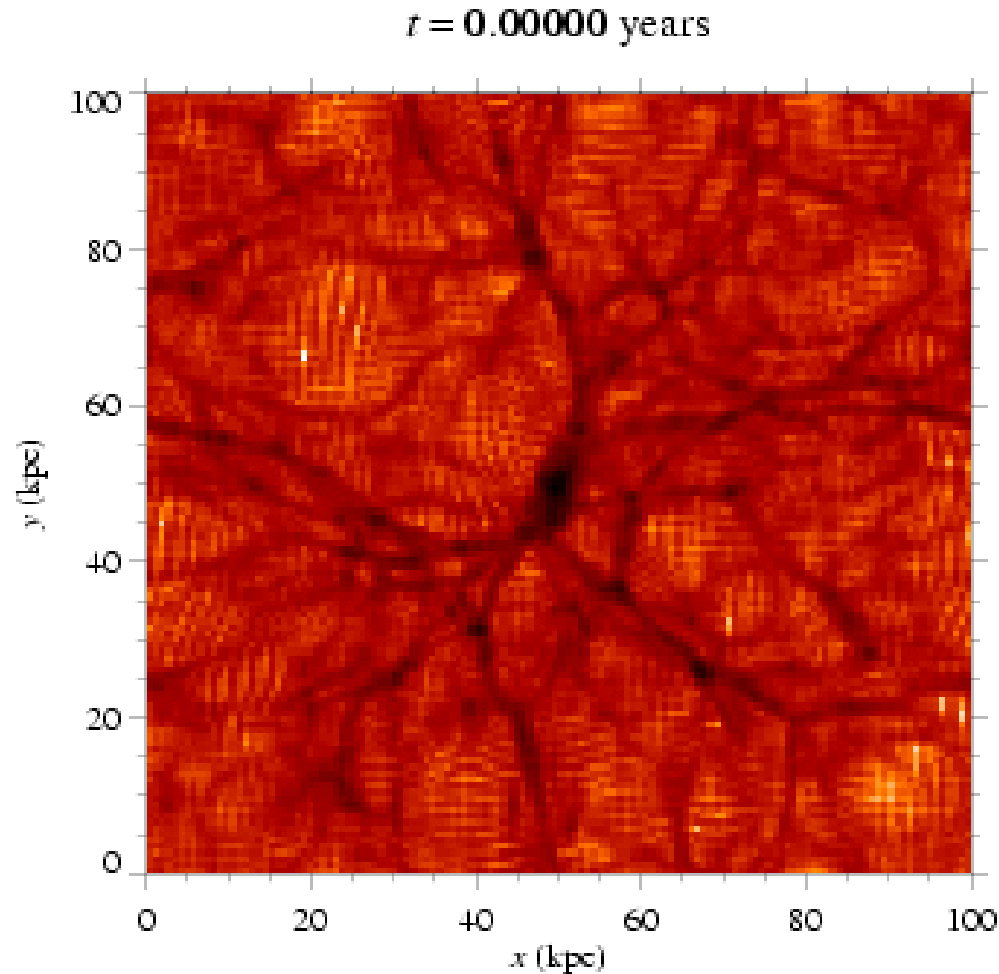
Cosmological I-front Evolution

1 Mpc box

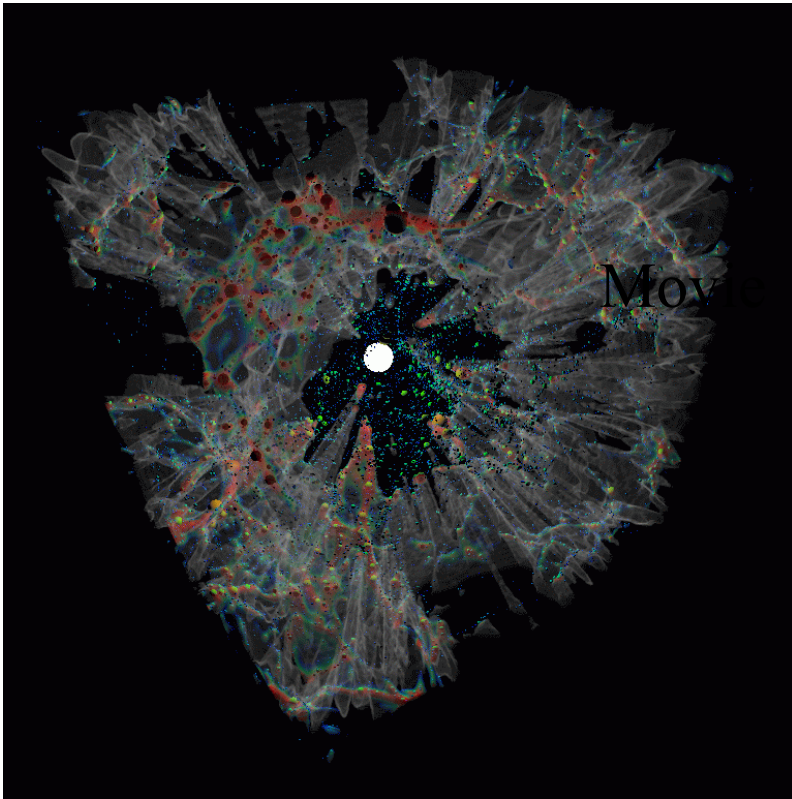
1 source

x-y cross-section

The evolution is complex (neither low-density first, not high-density first) dense filaments and halos cast long shadows



I-front propagation in a cosmological density field with minihalos



Visualization of an
I-front propagation in a
cosmological density
field (LCDM)

box : 0.5/h Mpc

redshift: $z=9$

Movie

THE PHOTOEVAPORATION OF MINIHALOS OVERTAKEN BY COSMOLOGICAL I-FRONTS

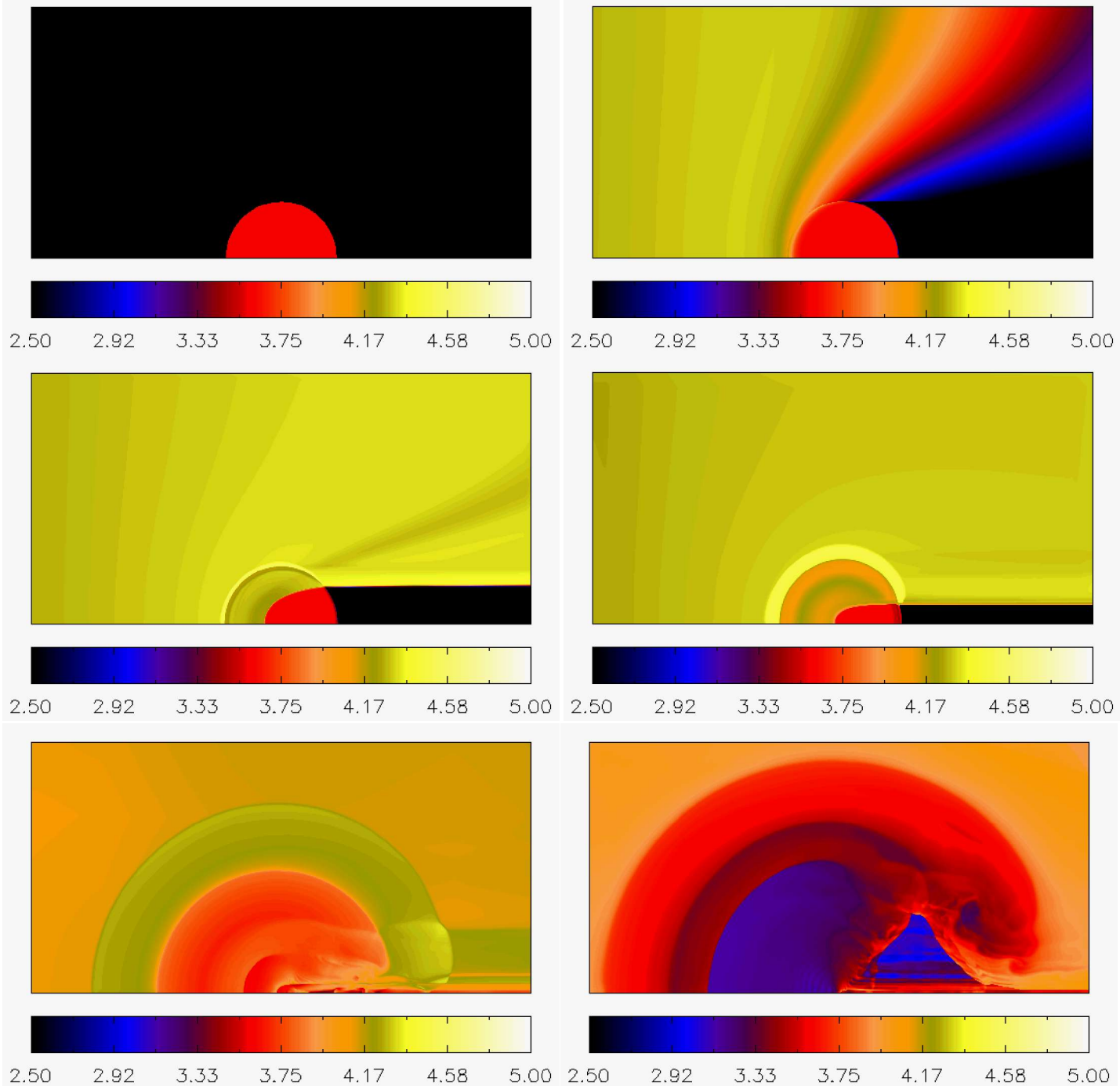
(Shapiro, Iliev & Raga 2004, Iliev, Shapiro and Raga 2005)

- Minihalo model: Truncated, nonsingular, isothermal sphere (“TIS”) of CDM + baryons + self-similar, spherical, cosmological infall. e.g. $M_{\text{tot}} = 10^7 M_{\text{sun}}$, $T_{\text{vir}} = 4000 \text{ K}$, $\alpha_v = 5.2 \text{ km/s}$, $r_t = 0.75 \text{ kpc}$, if $z_{\text{collapse}} = 9$.
- Halo masses: $M_0 = 10^4 - 4 \times 10^7 M_{\text{sun}}$
($4 \times 10^7 M_{\text{sun}}$ corresponds to $T_{\text{vir}} = 10^4 \text{ K}$ for $z_{\text{coll}} = 9$).
- Three Source Spectra:
 - (1) QSO-like: $F_v \propto v^{-1.8} (v > v_H)$
 - (2) Stellar (Pop II): Blackbody $T_{\text{eff}} = 50,000 \text{ K}$
 - (3) “No Metals” Stellar (Pop III): $T_{\text{eff}} = 100,000 \text{ K}$.
- Source turn-ons at $1+z_{\text{initial}} = 7-20$.
- Flux levels: $F_0 = N_{\text{ph},56} (v > v_H) / r_{\text{Mpc}}^2 = (0.01-10^3)$.
- 2D, axisymmetric, Eulerian hydro code with Adaptive Mesh Refinement and the van Leer flux-splitting algorithm, including radiative transfer (H, He bound-free opacity) (Raga et al. 1995, Mellema et al. 1998, Shapiro, Iliev & Raga 2004).
- Nonequilibrium ionization rate equations: H, He + (C, N, O, Ne, S) @ 10^{-3} solar abundance

Temperature at
times $t = 0.0, 0.2,$
 $2.5, 10, 60, 150$
Myrs.

$(M_{\text{halo}}, z_{\text{initial}}, F_0) =$
 $(10^7 M_{\text{sun}}, 9, 1).$

Pop II source.



Minihalo Photoevaporation Movies

Pop. II stars

temperature

gas number density

H I fraction

Pop. III stars

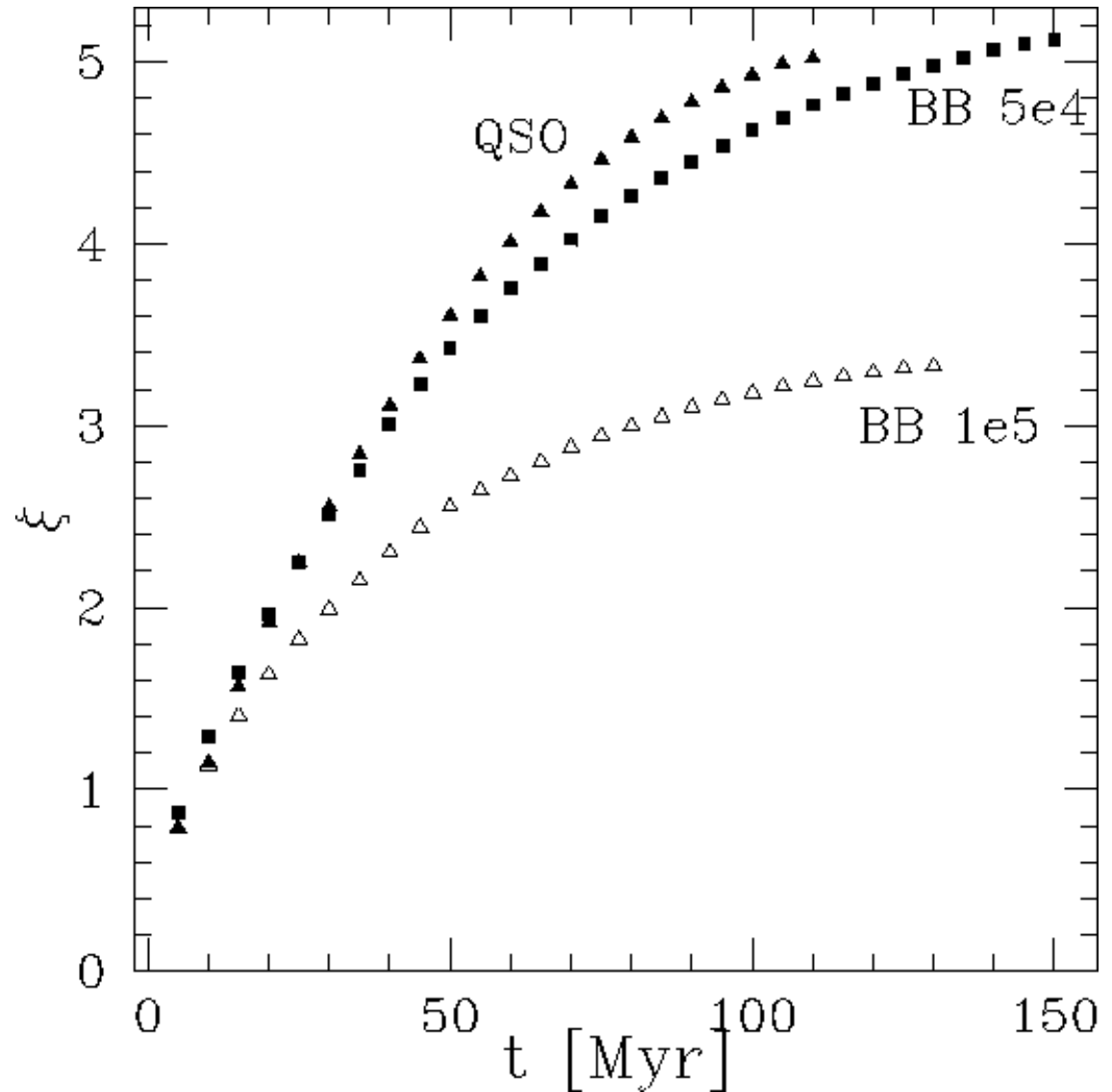
temperature

gas number density

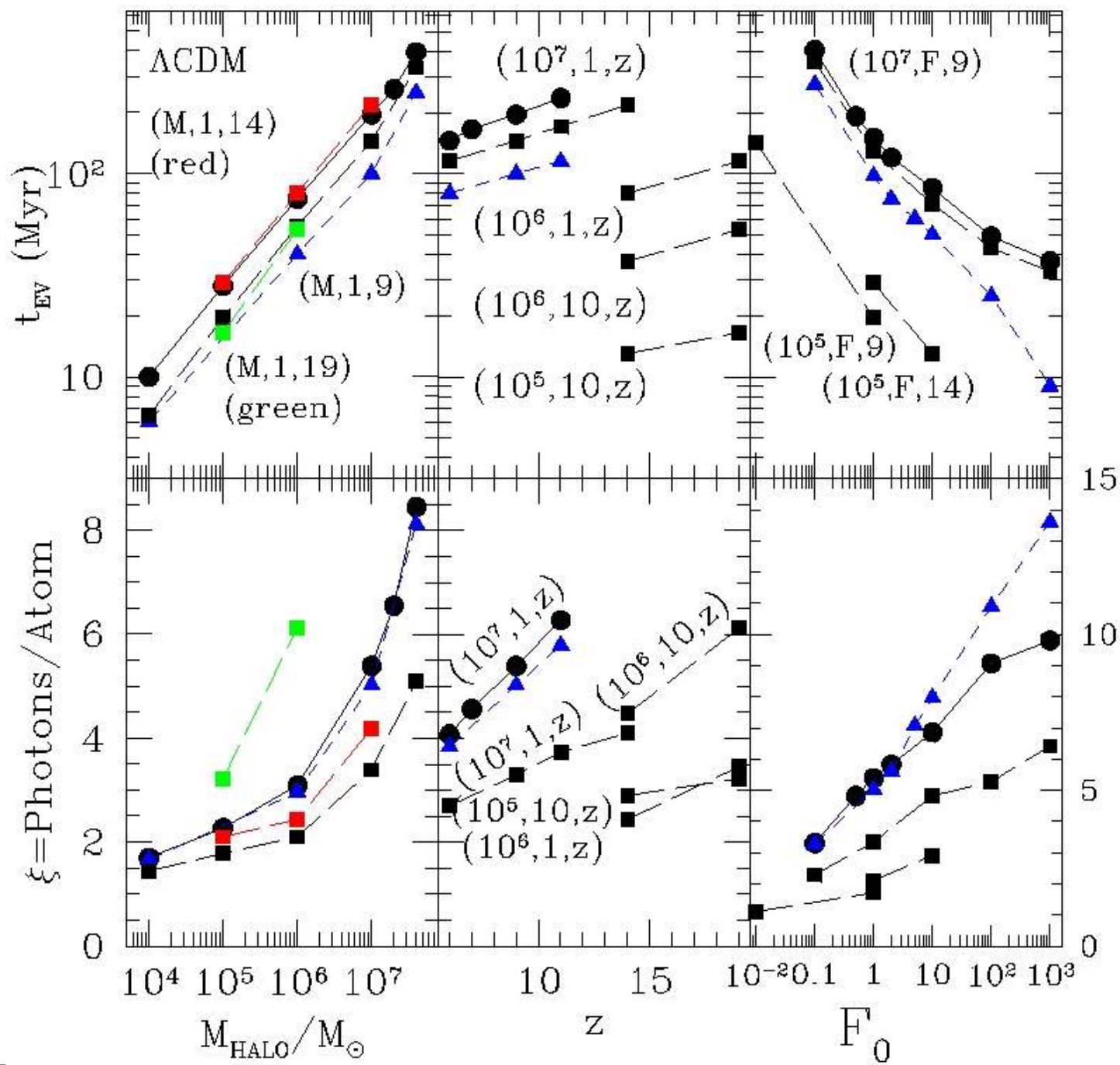
H I fraction

Ionizing Photons Consumed Per Minihalo Atom

- $\xi(t)$ = # photons consumed per H atom after time t .
- $(M_{\text{halo}}, z_{\text{initial}}, F_0) = (10^7 M_{\text{sun}}, 9, 1)$.



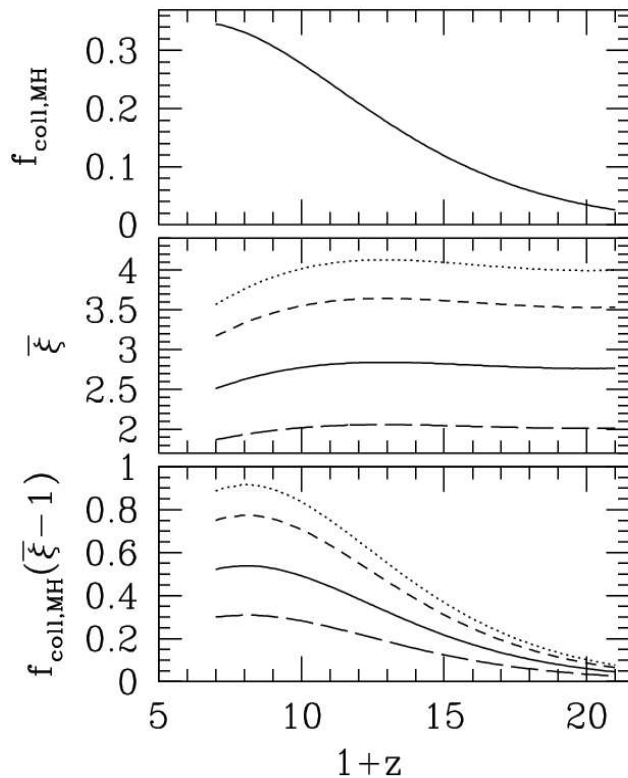
Evaporation times



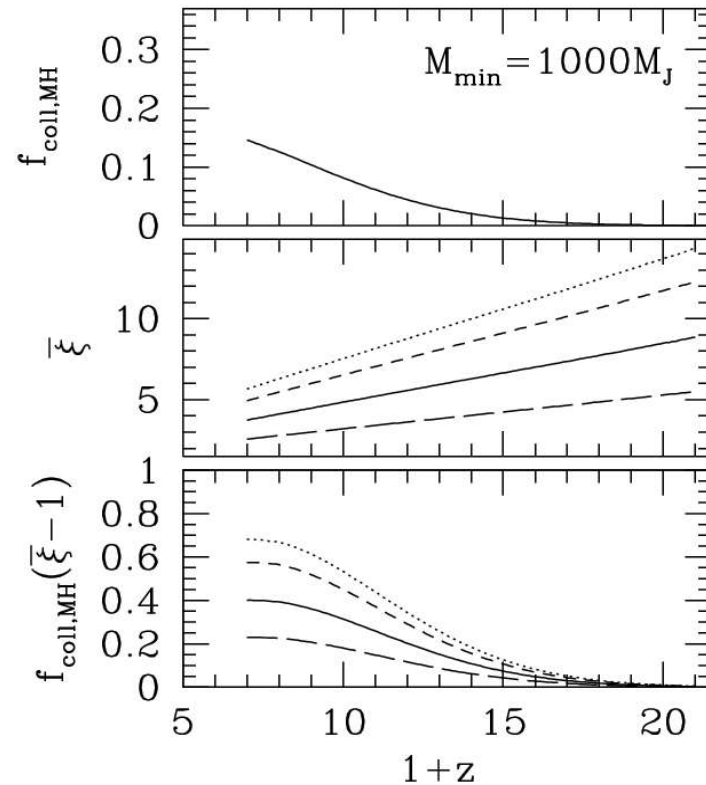
Ionizing photon consumption

Effect of Minihalos on Global Ionizing Photon Consumption: A Rough Estimate

No reheating

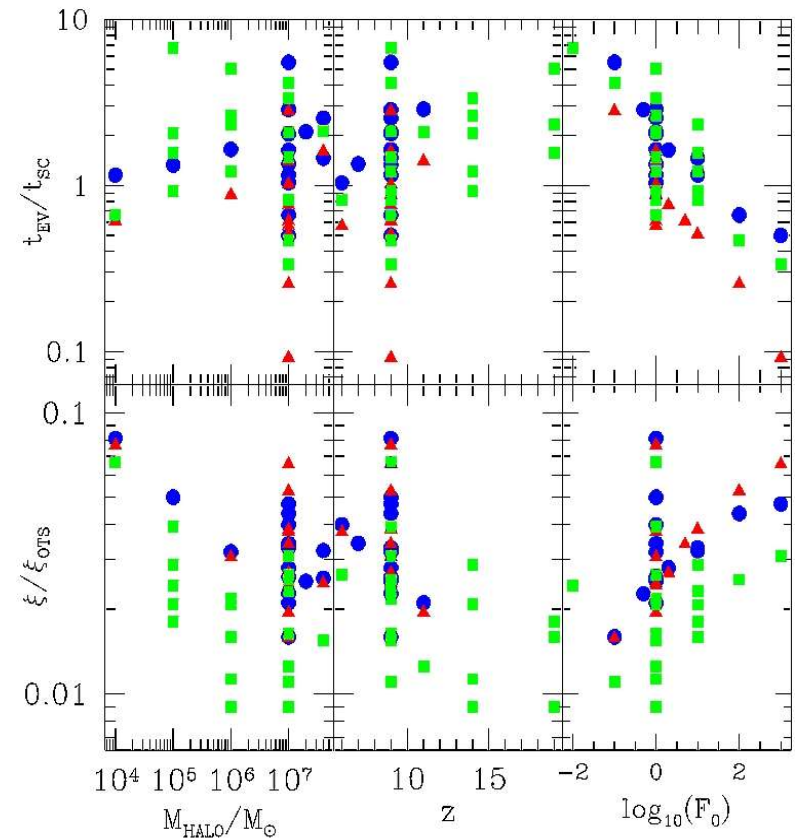


With reheating

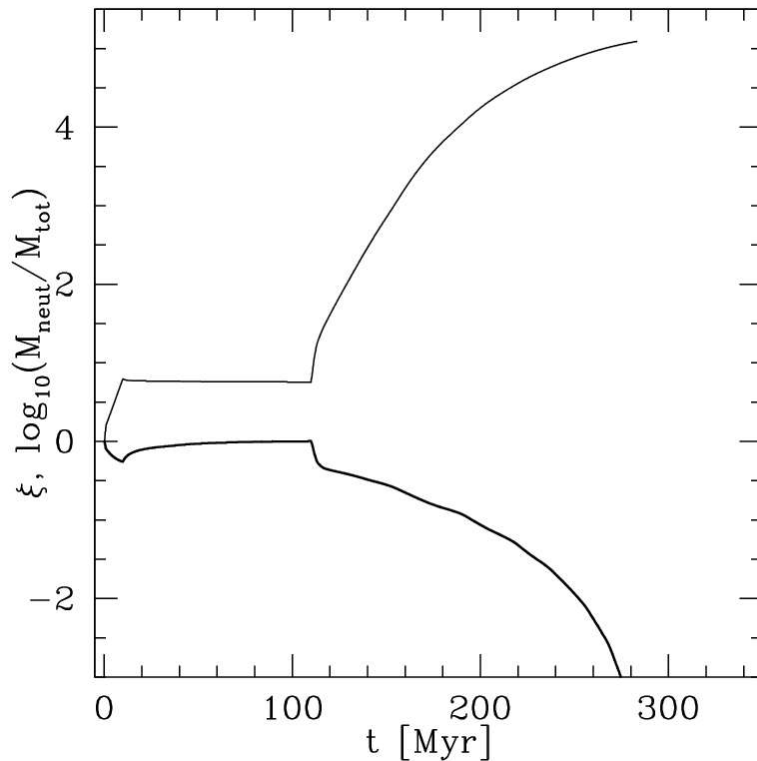


Comparison to Optically-Thin, Static Prediction

- Haiman, Abel & Madau 00 obtained photon consumption and evaporation time by assuming minihalo is optically-thin and static during its evaporation, which happens on sound-crossing time, no dependence on ionizing flux or its spectrum
 - both estimates are incorrect
 - evaporation time could be off by up to order-of-magnitude up or down
 - consumption is too high by 1-2 orders-of-magnitude
- => both RT and dynamics are important for this problem



Case of Intermittent Ionizing Sources

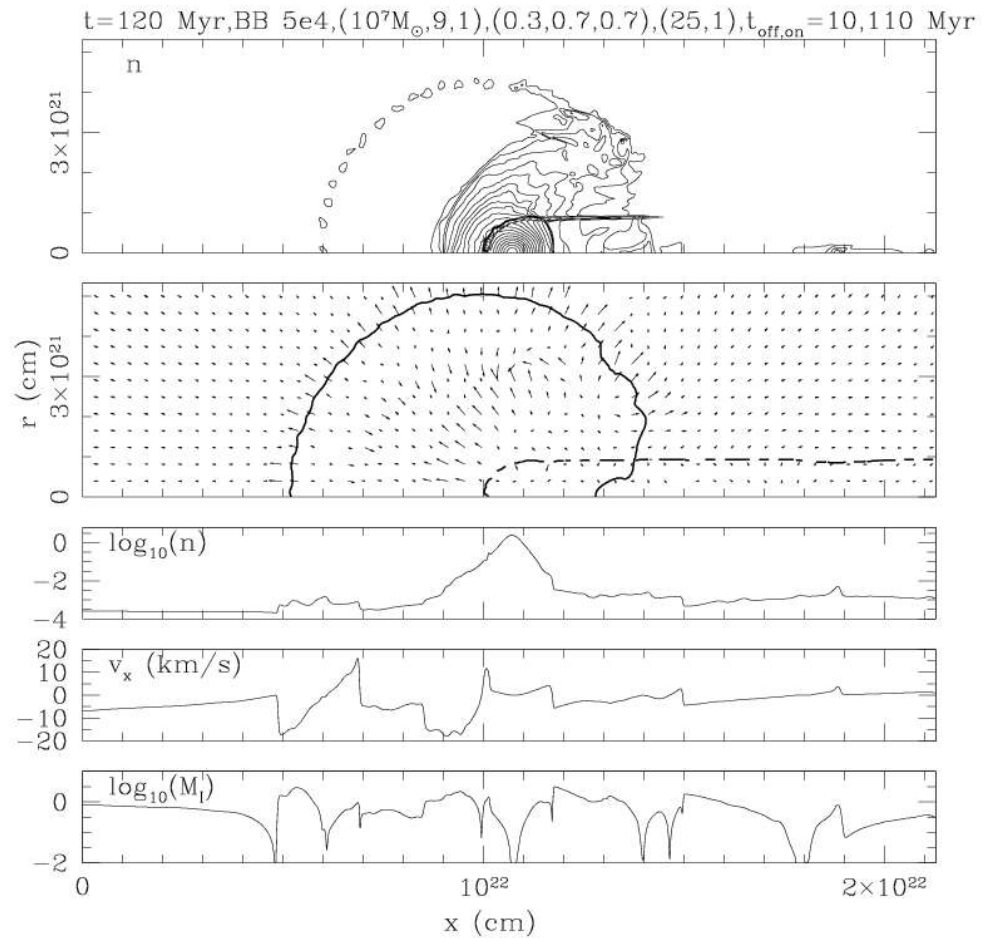
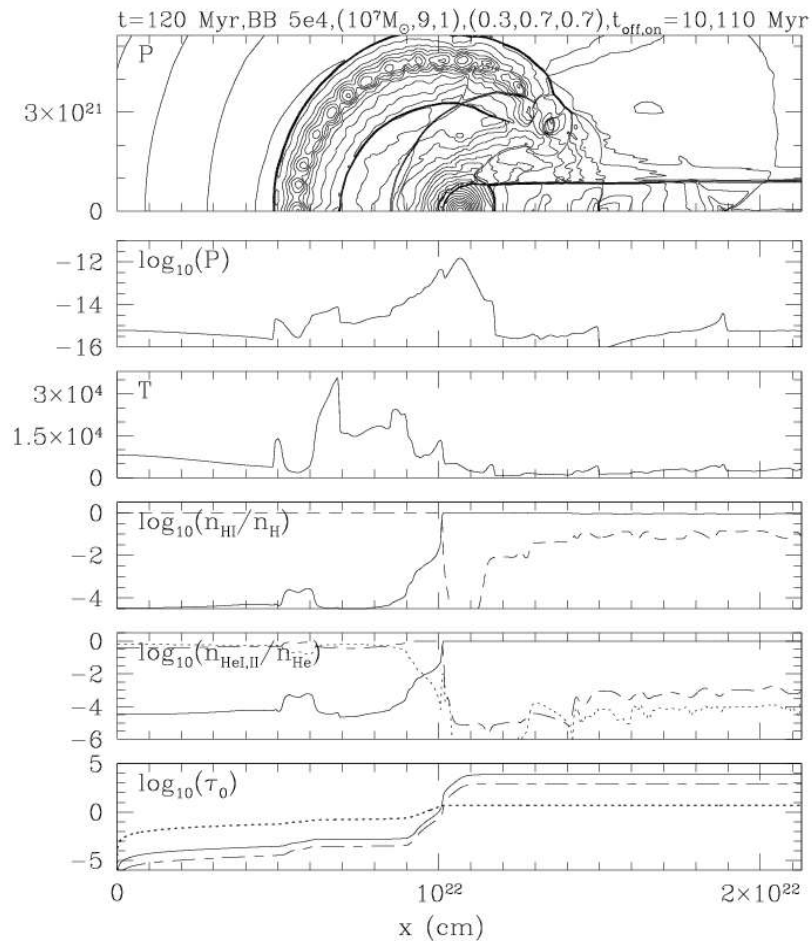


Ionizing source on for 10 Myr, off for 100 Myr and on again.

Results:

evaporation time is longer by about 80 Myr, while photon consumption is very similar to case of uninterrupted source with same flux.

Case of Intermittent Ionizing Sources, $t=120$ Myr

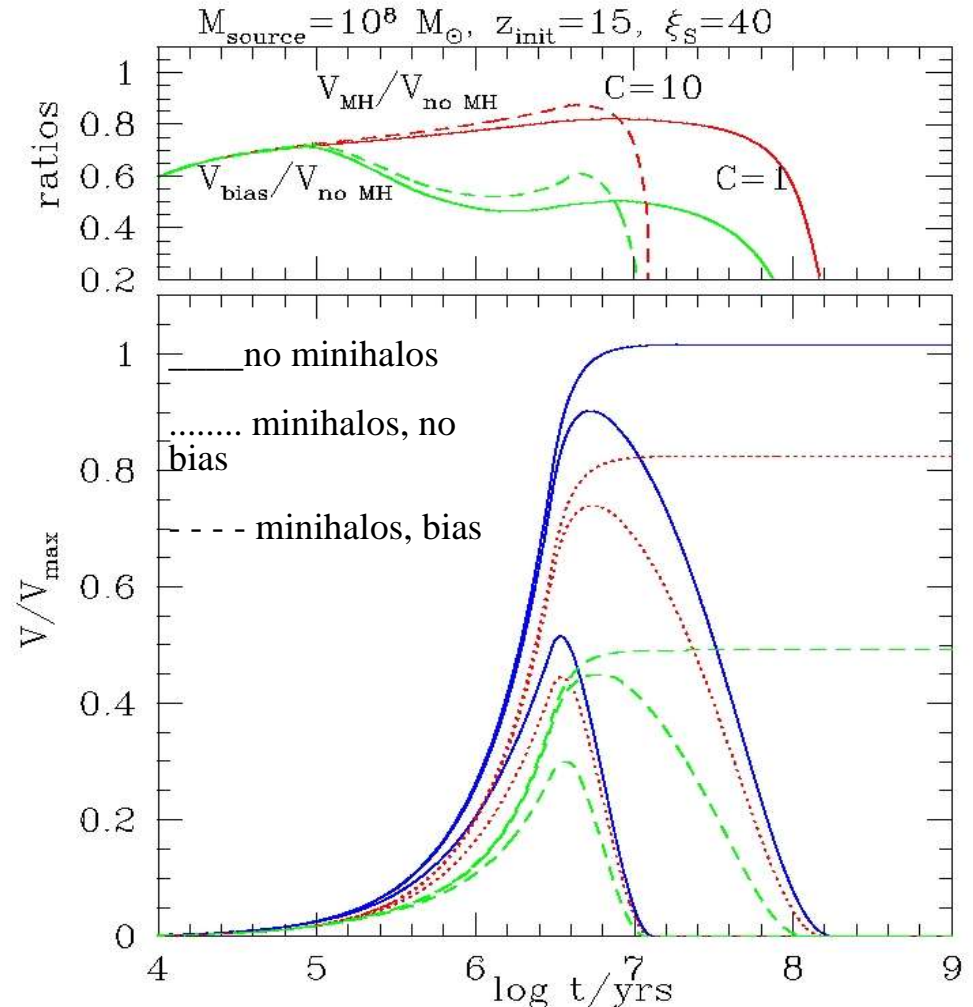


Effect of minihalos on the propagation of a cosmological I-front

(Iliev, Scannapieco & Shapiro 2005)

Propagation of an I-front about an individual source:

$10^8 M_{\text{solar}}$ source forming at $z=15$ producing 40 photons/atom during its lifetime



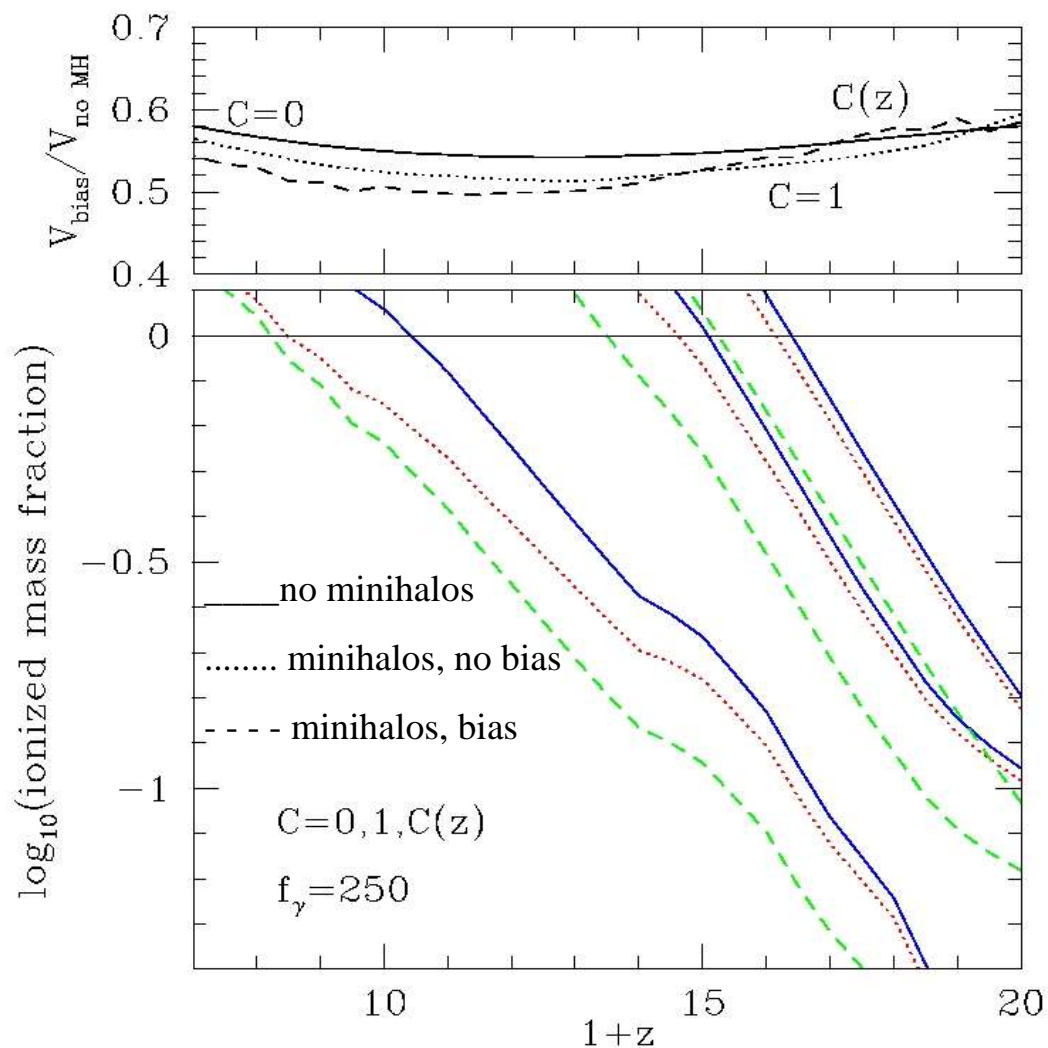
Effect of Minihalos and IGM Clumping on Reionization

Let each source halo create its own expanding spherical H II region.

I-front speed is slowed by minihalo trapping and evaporation and recombinations in IGM.

Integrate over statistical distribution of source halo masses and turn-on epochs until neighboring H II regions overlap => reionization finished.

Minihalos can increase photon consumption by factor of ~ 2 , delaying reionization by $z \sim 2$.

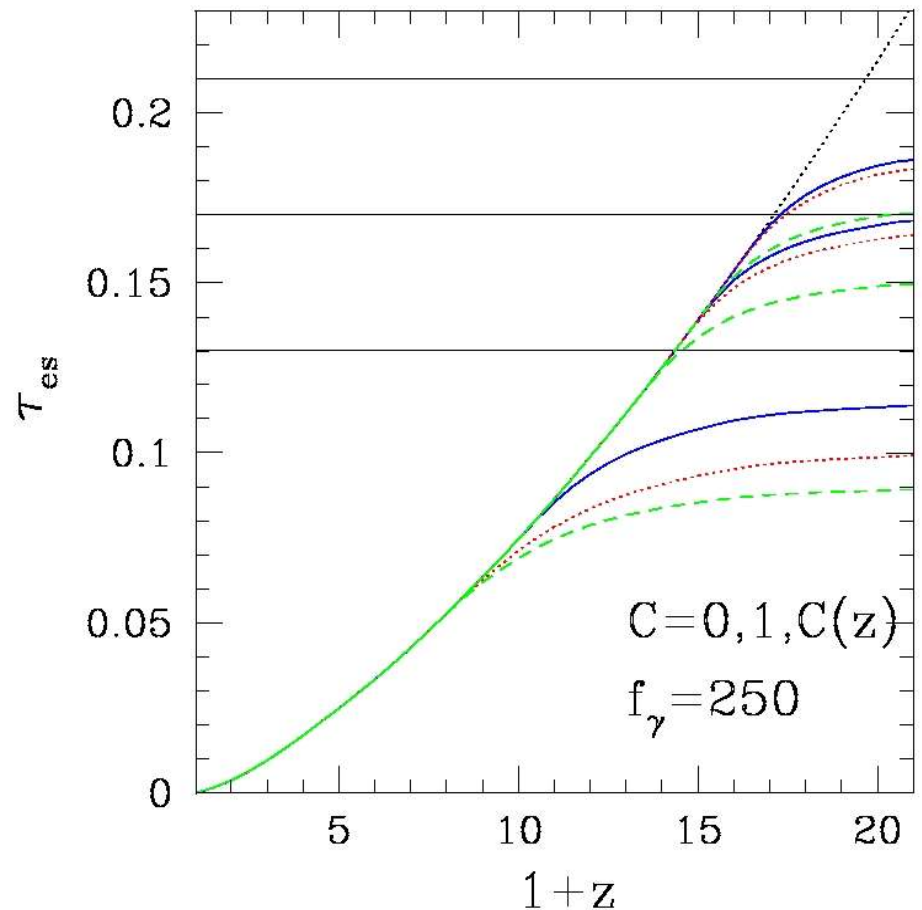


Effect of Minihalos and IGM Clumping on Reionization II: Electron Scattering Optical Depth

Multiple models studied (see paper for details)

For sources producing a total of 250 photons per baryon during their lifetime:

- Consistent with WMAP constraint for low or no clumping of IGM
- Produces somewhat low optical depth for cosmologically-evolving IGM clumping



Observing the Dark Ages and Reionization at 21-cm of Hydrogen

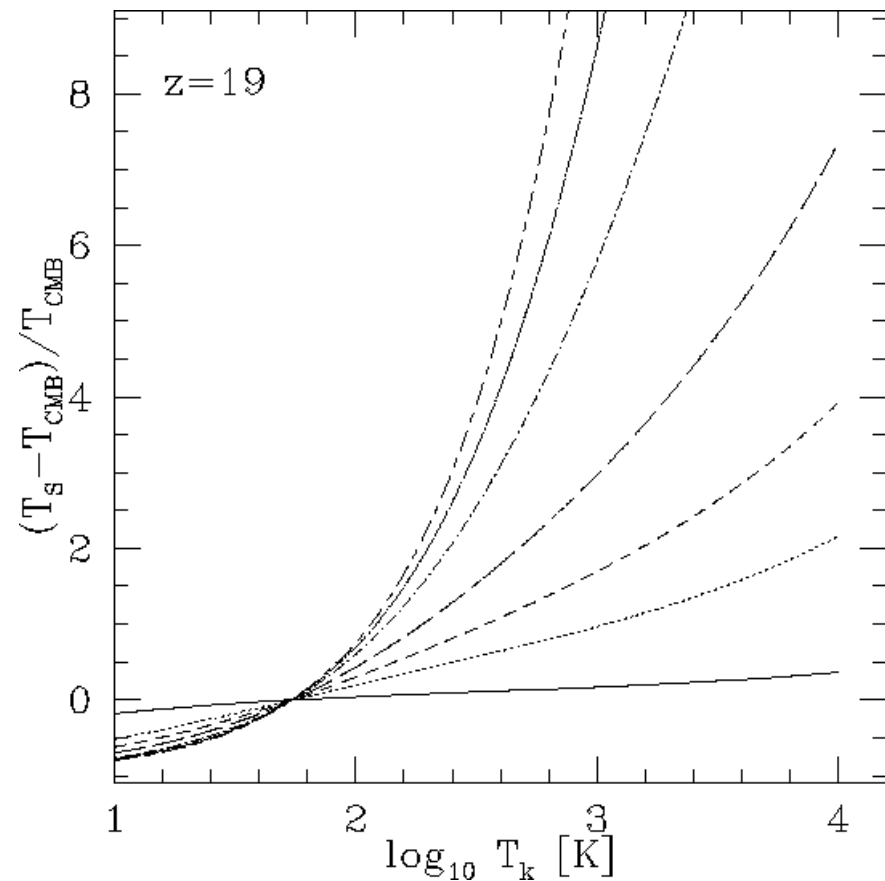
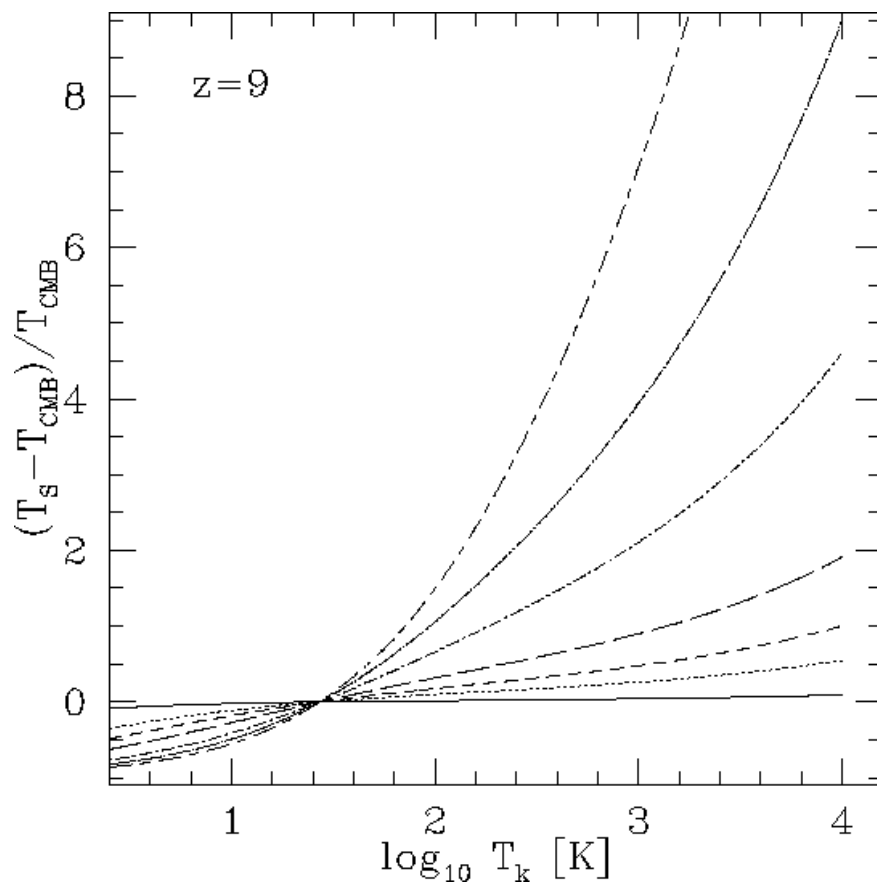
Decoupling the Spin Temperature of 21-cm Transition from the CMB

Spin temperature determined by balance between collisional and radiative excitation and de-excitation by atoms and by CMB and Ly- α photons:

$$T_S = \frac{T_{\text{CMB}} + y_c T_K + y_\alpha T_\alpha}{1 + y_c + y_\alpha}$$

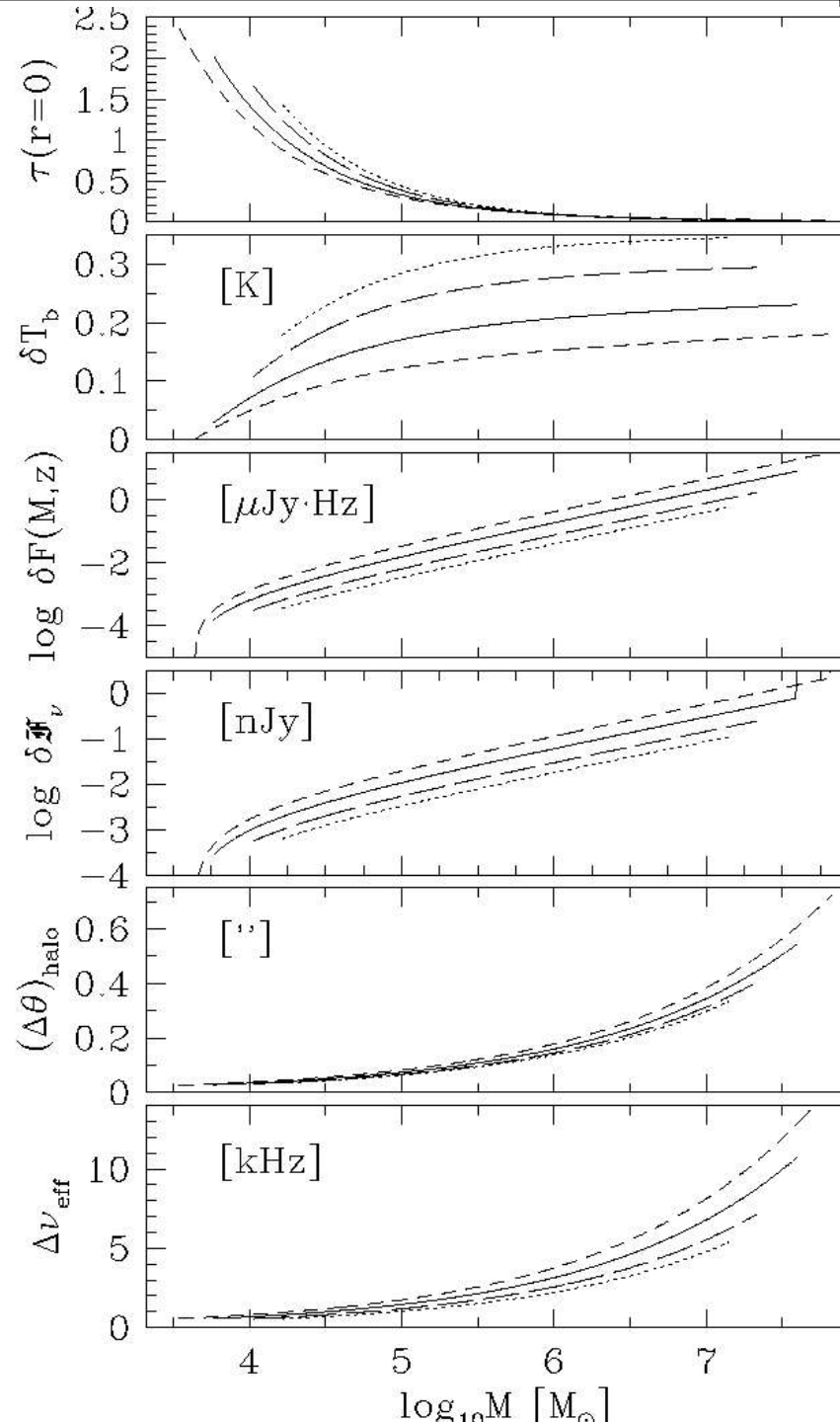
Collisional decoupling of T_s from T_{CMB} for different overdensities with respect to mean IGM.

bottom to top : $\delta = 0, 5, 10, 20, 50, 100$ and 200 at $z=9$ (left panel) and $z=19$ (right panel).



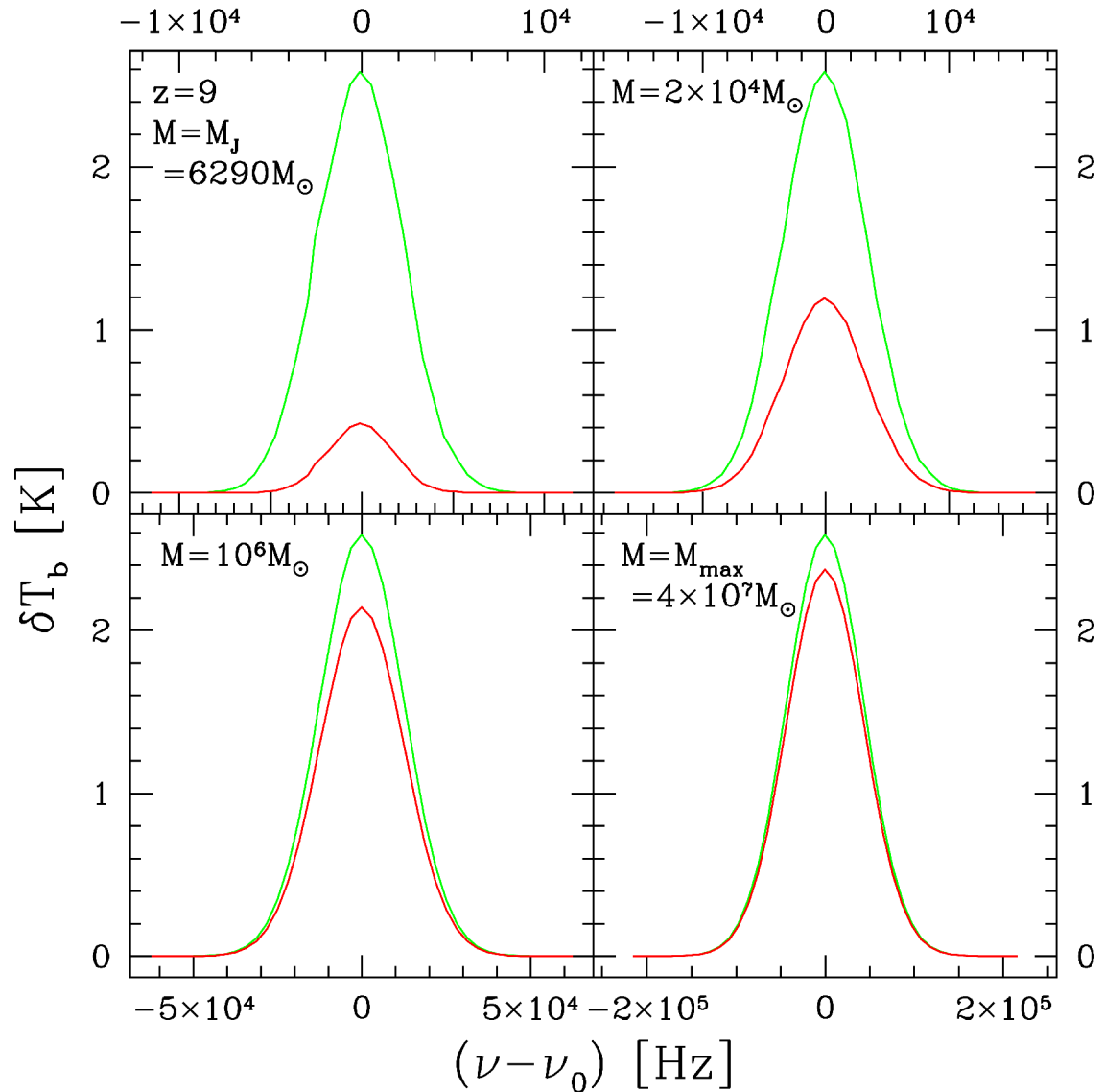
Individual minihalo emission lines

- › For $1 + z = 7$ (short-dashed), 10 (solid), 15 (long-dashed), and 20 (dotted) vs. minihalo mass M .
- › Optical depth $\tau_{\nu,0}(r = 0)$ through minihalo center at line-center frequency ν_0
- › Differential antenna temperature δT_b
- › line-integrated differential flux $F(M,z)$ relative to CMB
- › total differential flux per unit frequency $F_{\nu 0}$
- › angular size of minihalo $(\delta\theta)_{\text{halo}}$
- › redshifted effective width $\Delta\nu_{\text{eff}}(z)$ of the 21-cm line as observed at $z = 0$ at received frequency $\nu_{\text{rec}} = \nu_0(1 + z)^{-1}$.



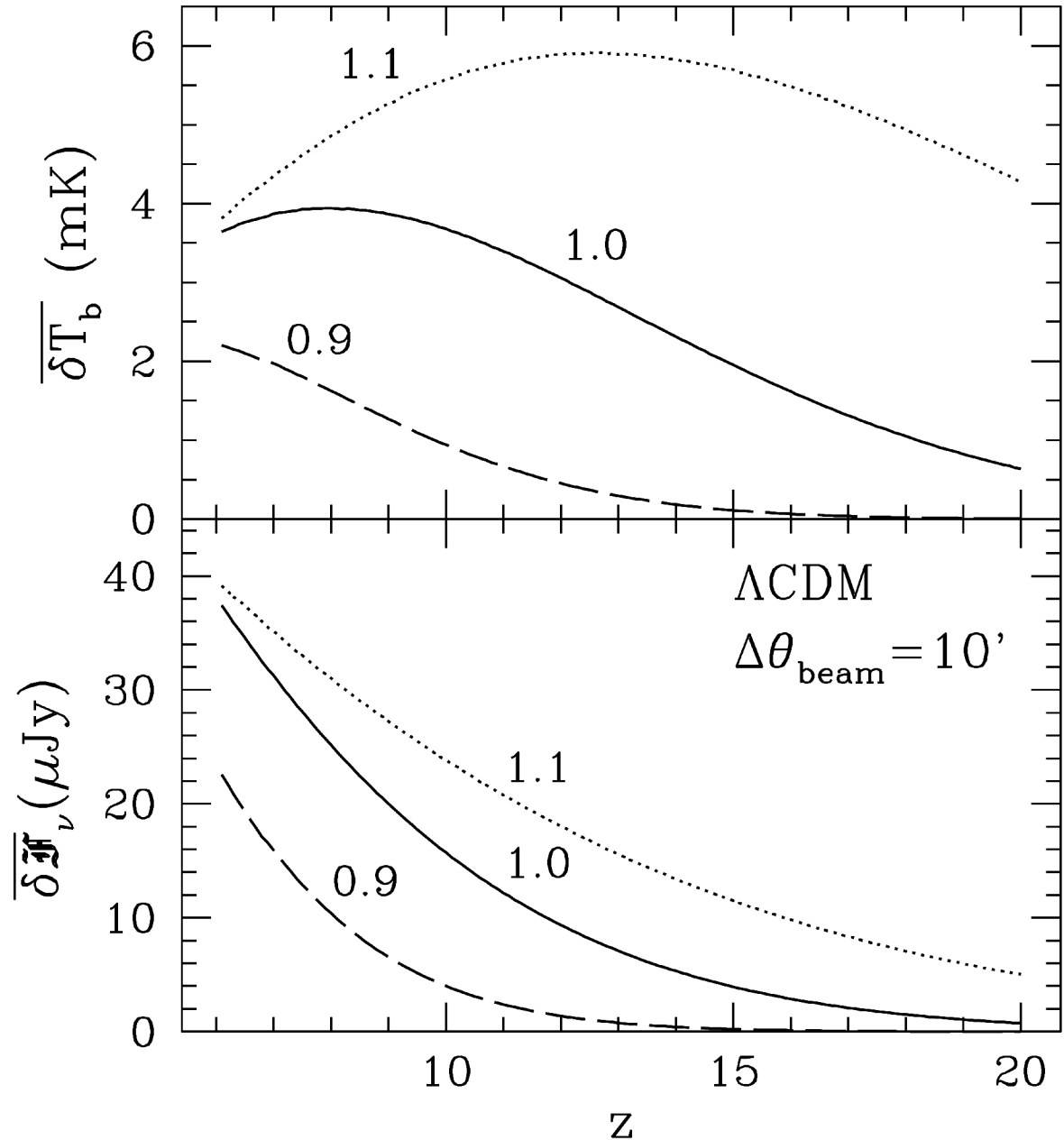
21-cm emission line profiles for individual minihalos of different mass at $z = 9$.

Differential antenna temperatures δT_b [K] versus emitted frequency ν_{em} for spatially unresolved halos, from detailed radiative transfer calculation (lower curves) and optically thin approximation (upper curves). Optical depth is important.



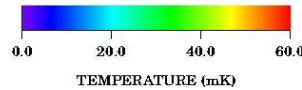
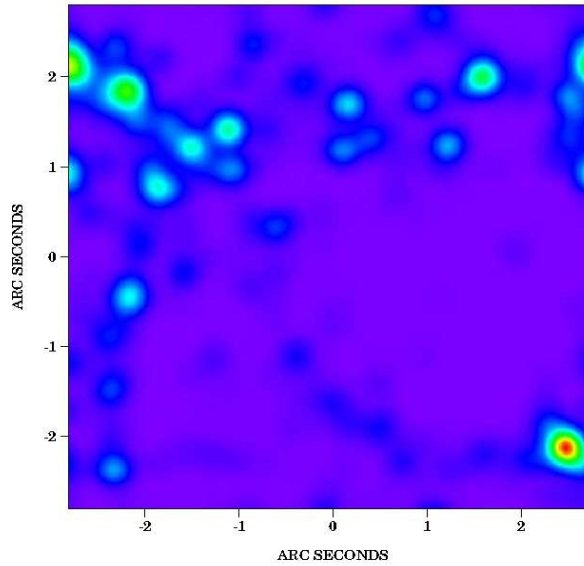
Minihalo radiation mean background.

Average observed differential antenna temperature $\overline{\delta T_b}$ and average differential flux per unit frequency $\overline{\delta \mathcal{F}_\nu}$ for beam size of $\Delta\theta_{\text{beam}} = 10'$ at the redshifted 21 cm line frequency due to minihalos vs. redshift z for Λ CDM models with power spectrum tilts $n_p = 0.9, 1.0, \text{ and } 1.1$, as labeled.

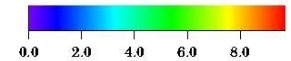
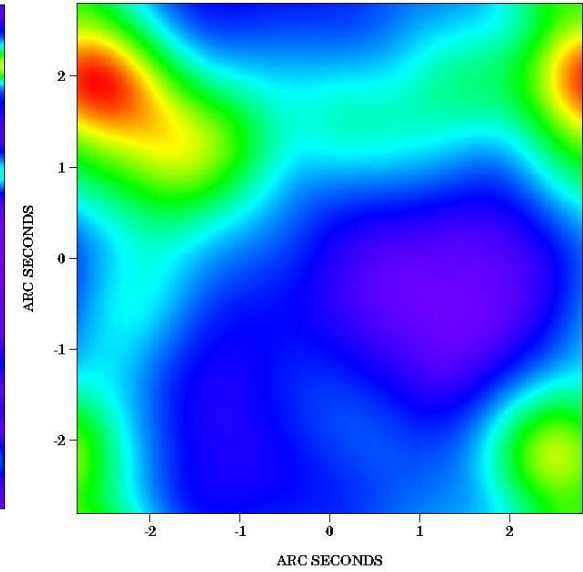


ANGULAR FLUCTUATIONS IN THE 21-CM EMISSION BACKGROUND. The clustering of minihalos as structure grows hierarchically in a CDM universe causes angular fluctuations in the 21-cm radiation background. To illustrate this, we have performed N-body simulations of halo formation in CDM. Radio maps of the 21-cm emission from the simulation cubes at $z = 9$ are shown.

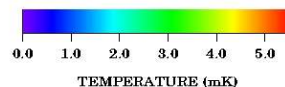
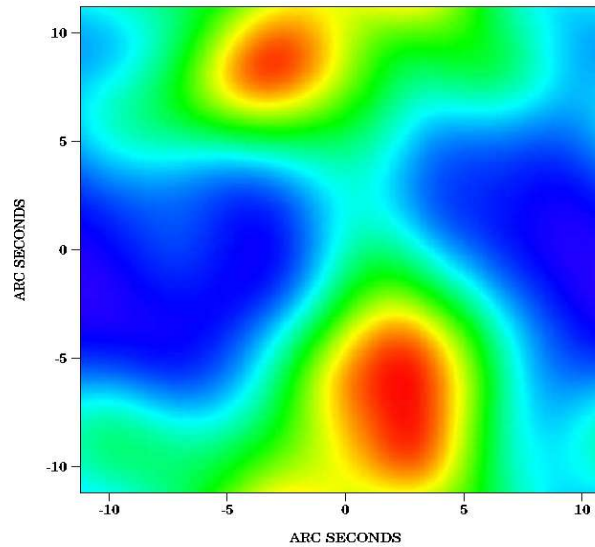
LCDM $Z = 9$ 0.25 MPC BOX (COMOVING) 0.25" BEAM



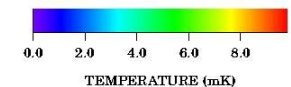
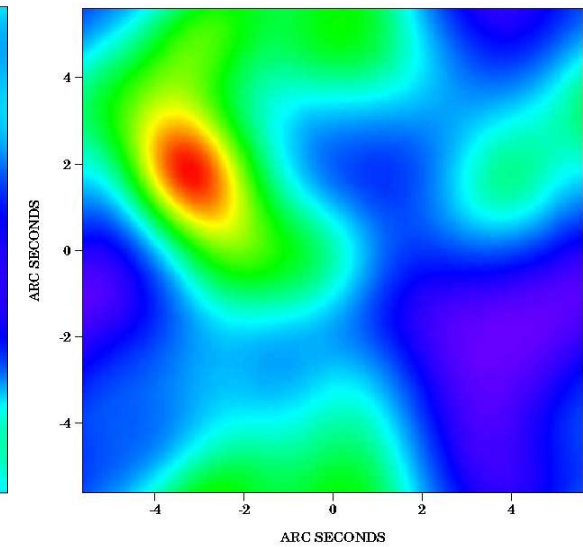
LCDM $Z = 9$ 0.25 MPC BOX (COMOVING) 1" BEAM



LCDM $Z = 9$ 1 MPC BOX (COMOVING) 4" BEAM



LCDM $Z = 9$ 0.5 MPC BOX (COMOVING) 2" BEAM



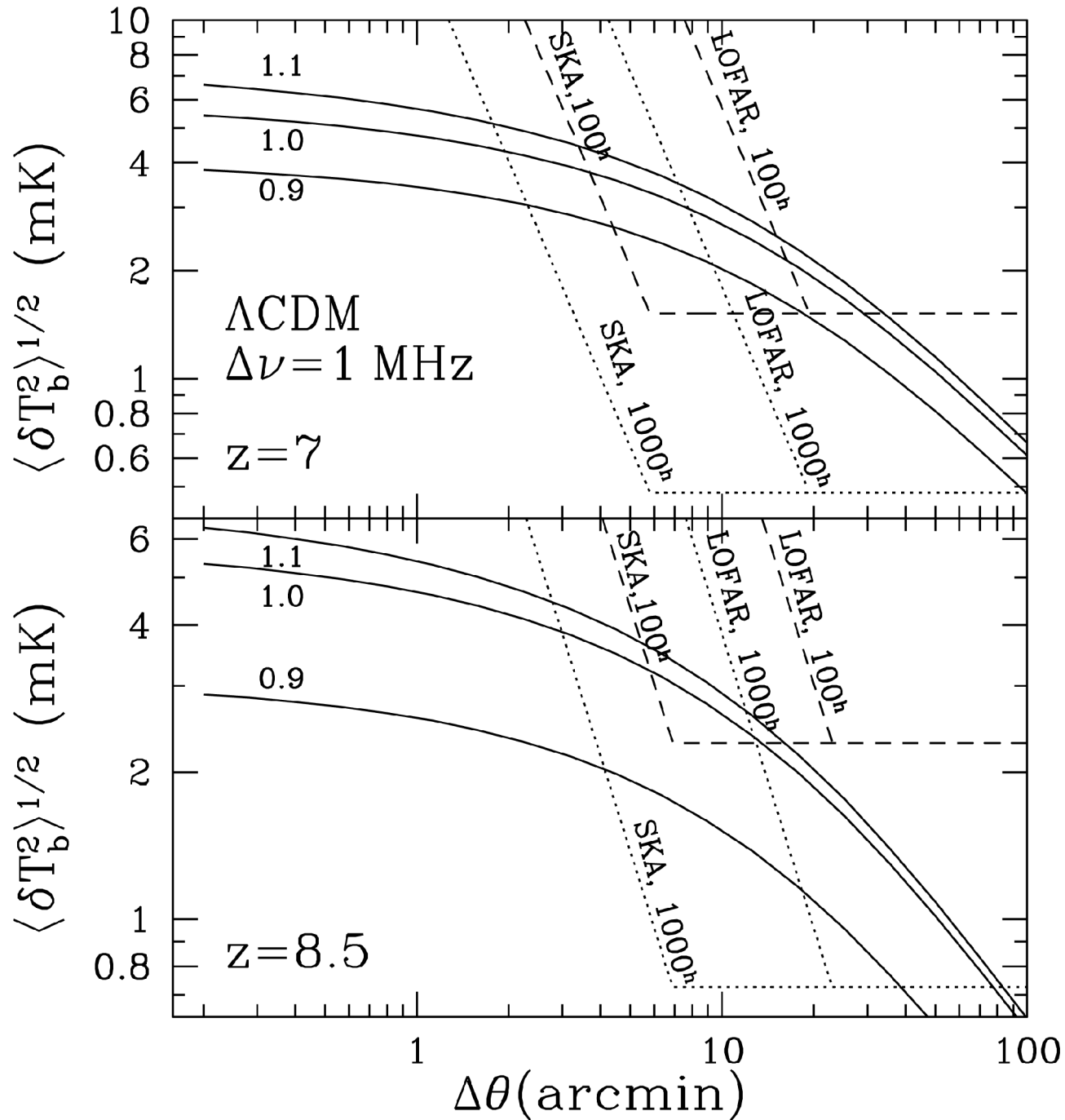
Predicted 3-differential antenna temperature fluctuations for different beam sizes.

Should be observable for:

$\geq 20'$ beam
(LOFAR)

$\geq 7'$ beam (SKA)

and > 100 h
integration



Predicted 3- σ
differential antenna
temperature
fluctuations for
different redshifts.

Observable for:

25' beam (LOFAR,
SKA):

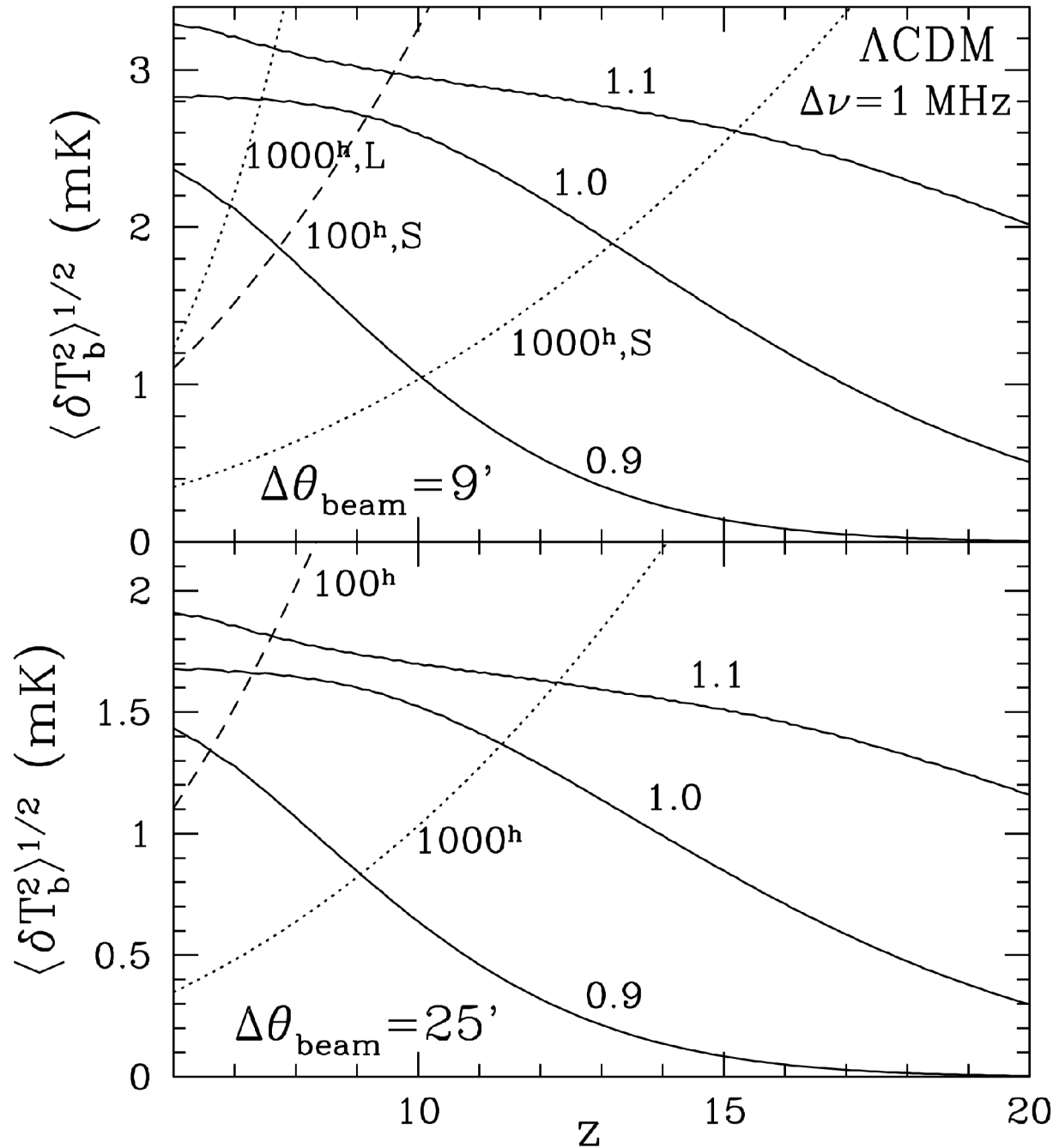
$z \sim 6-7.5$ (100 hours)

$z \leq 11.5$ (1000 h)

9' beam (SKA):

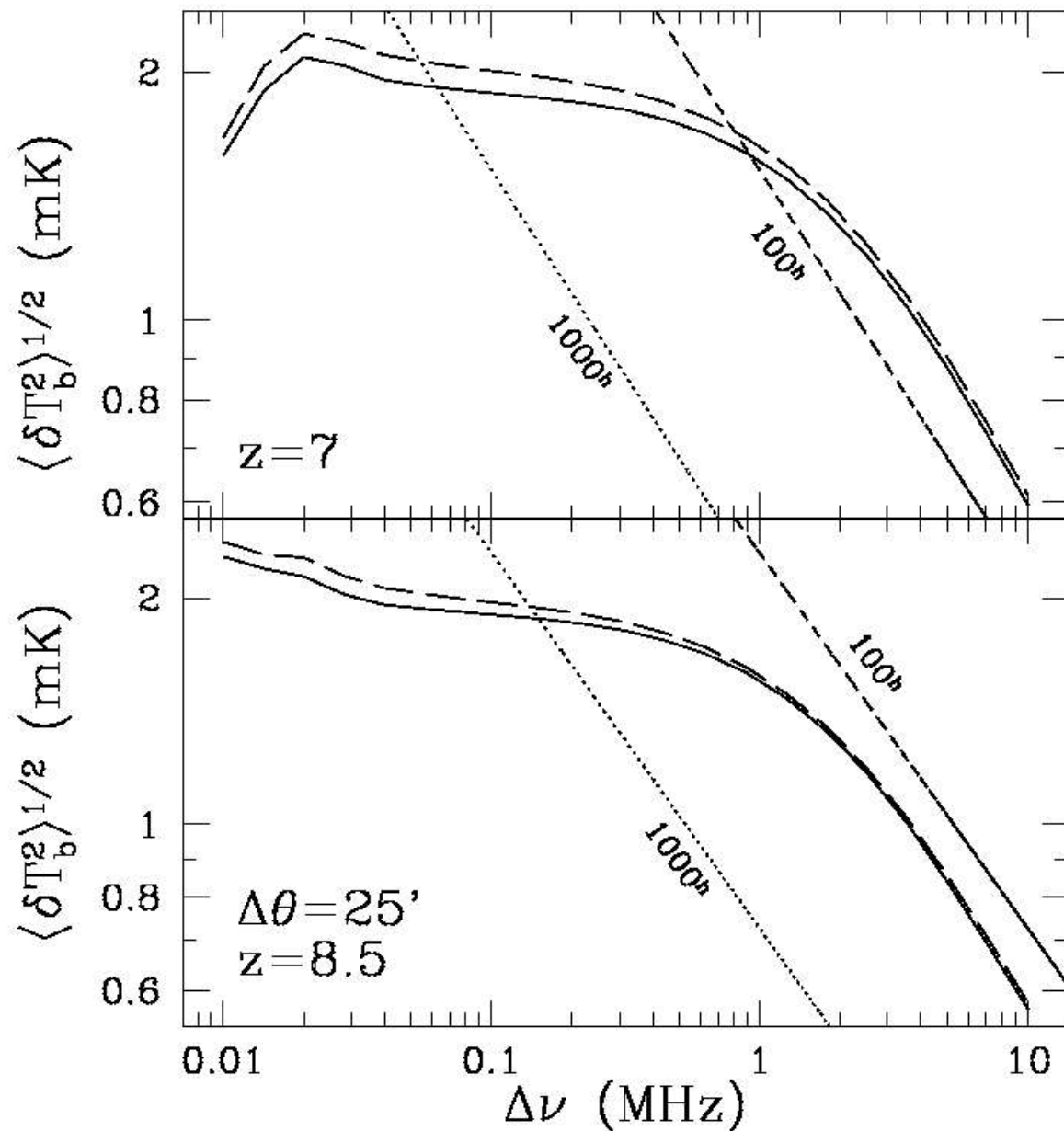
$z \leq 9$ (100 hours)

$z \leq 13$ (1000 h)



Optimal bandwidth
for LOFAR or SKA
(for beam size of
25')

$\Delta\nu \sim 1\text{-}2\text{ MHz}$

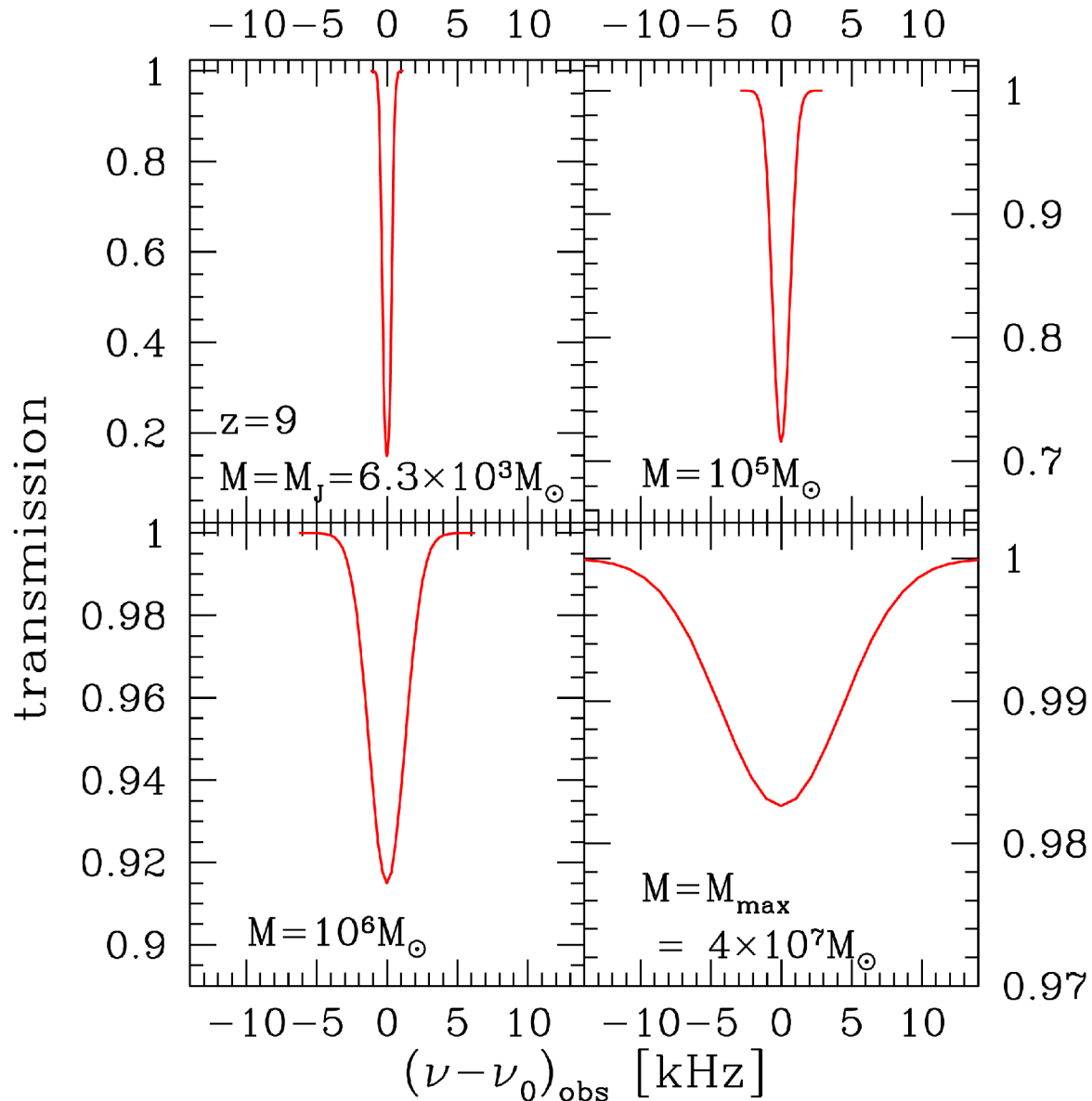


Minihalo Absorption lines

LOS 21-cm absorption line profiles for individual minihalos at $z = 9$.

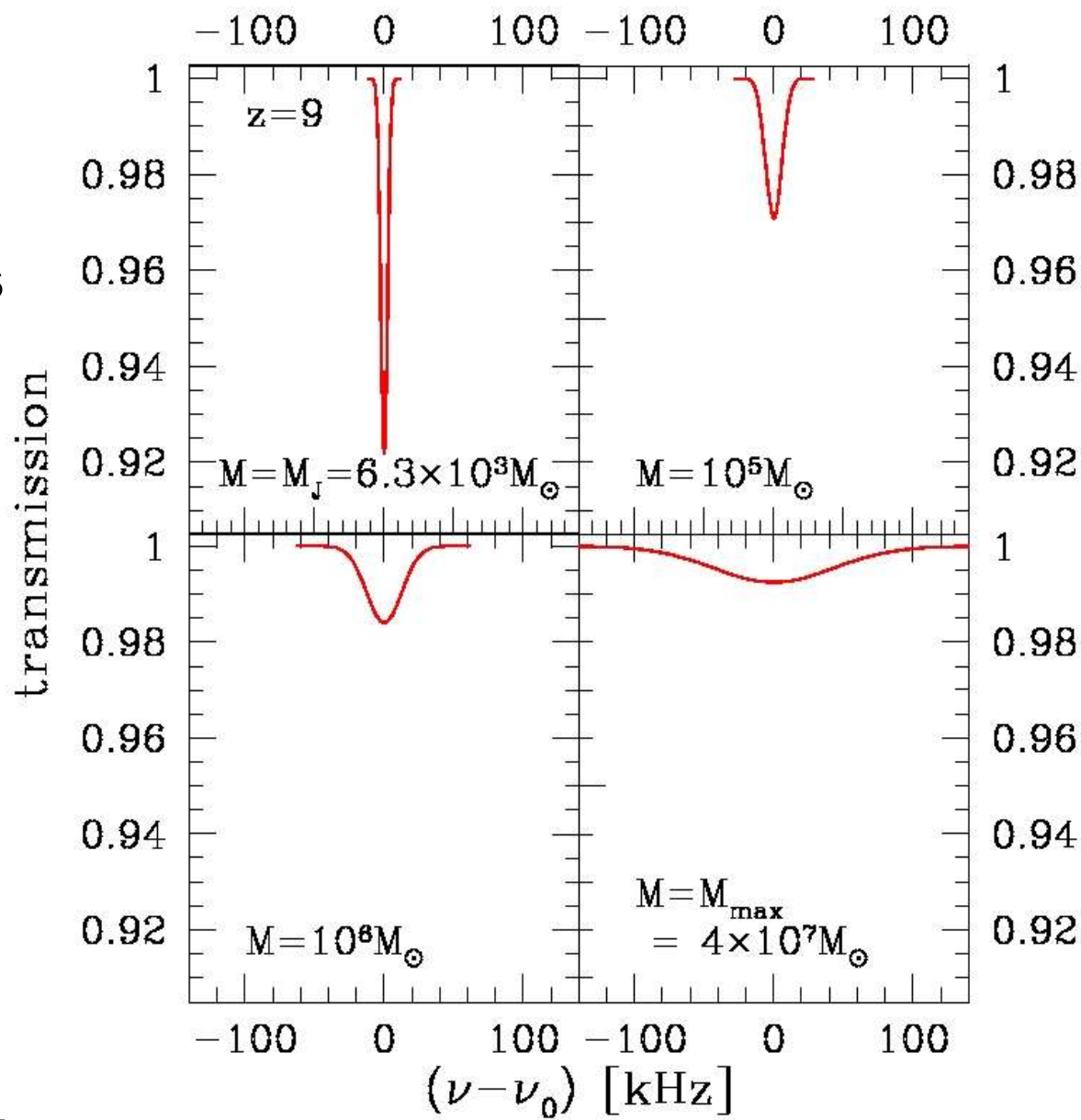
Transmission factor versus received frequency ν_{rec} at $z = 0$, for LOS with zero impact parameter)

(see also Furlanetto & Loeb 02).



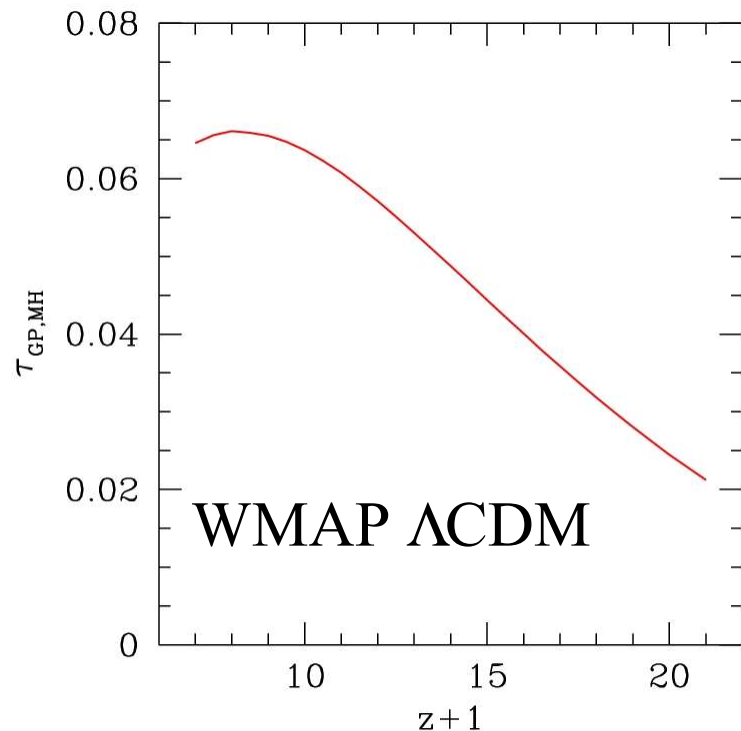
Face-averaged 21-cm absorption line profiles for individual minihalos at $z = 9$.

Transmission factor
versus received
frequency ν_{rec} at $z = 0$.



21-cm absorption line opacity from MHs (21-cm GP effect)

- minihalos create a “21-cm forest” of absorption lines, similar to Ly- α at lower z
- if lines are unresolved, they create mean opacity which is significant and should be detectable if significantly strong background radio sources exist, as expected.

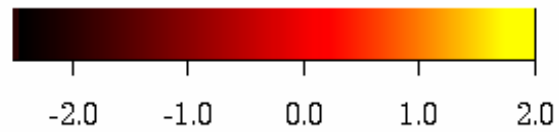
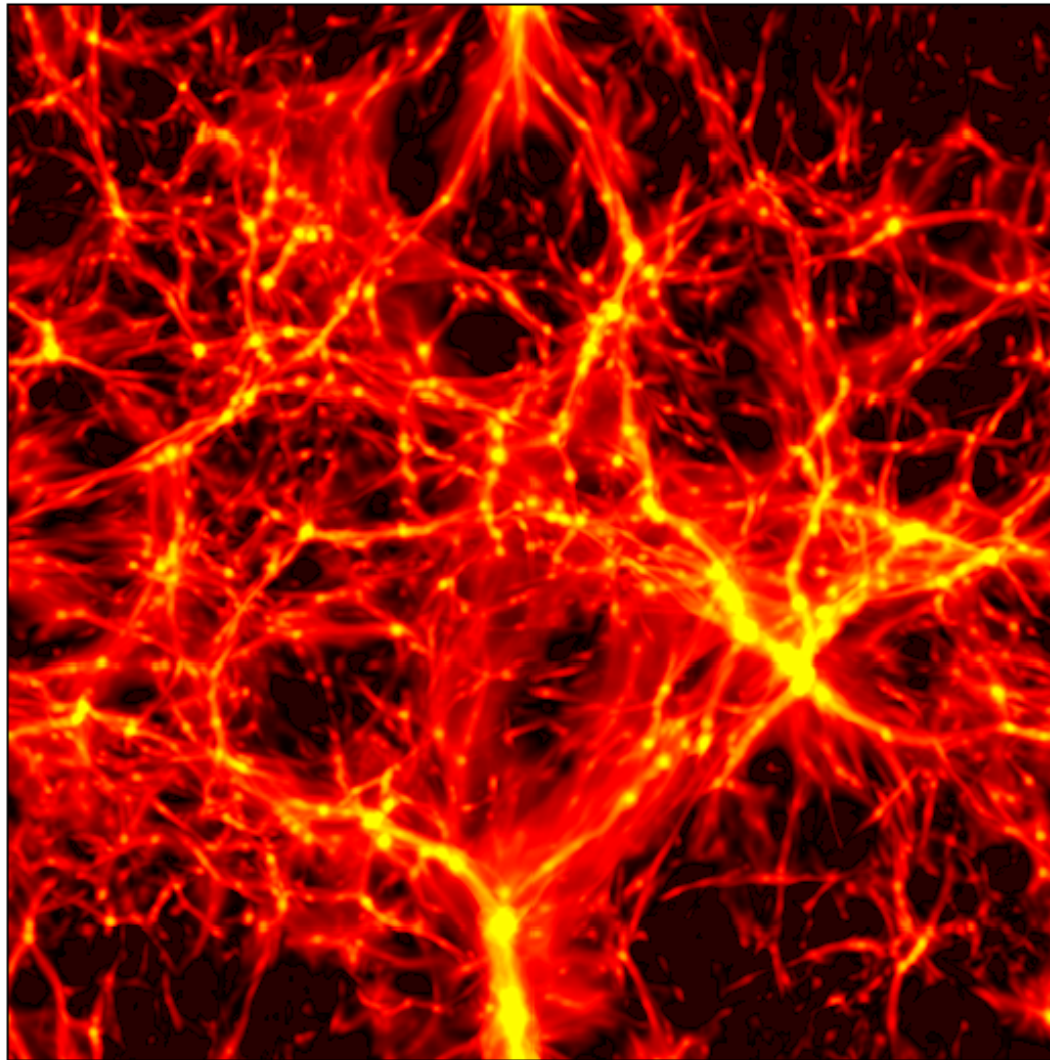


21-cm Emission from Minihalos vs. Shock-heated Gas outside Virialized Regions

(Shapiro et al., in prep.)

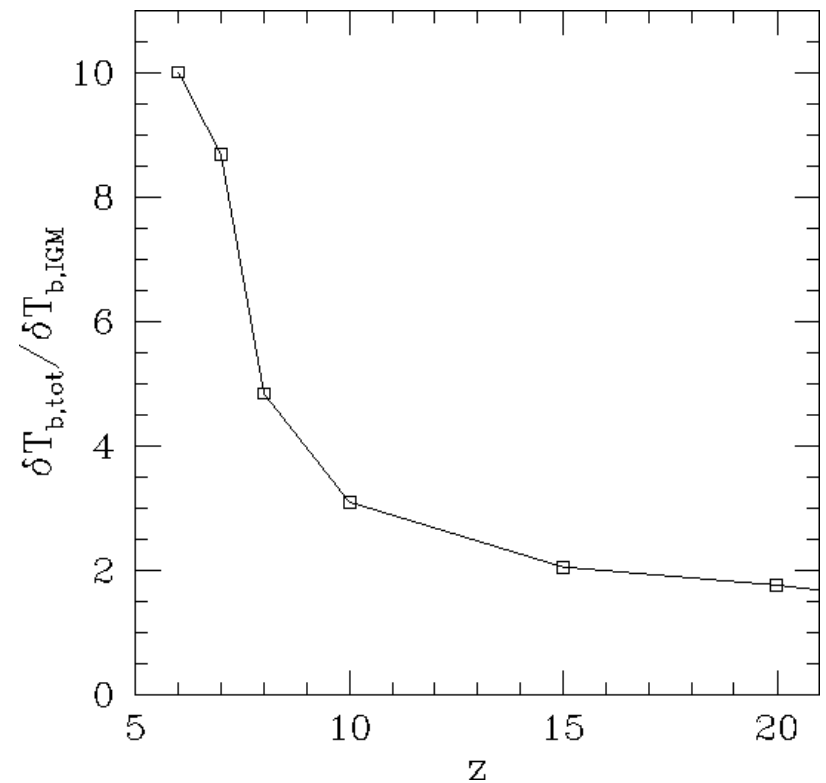
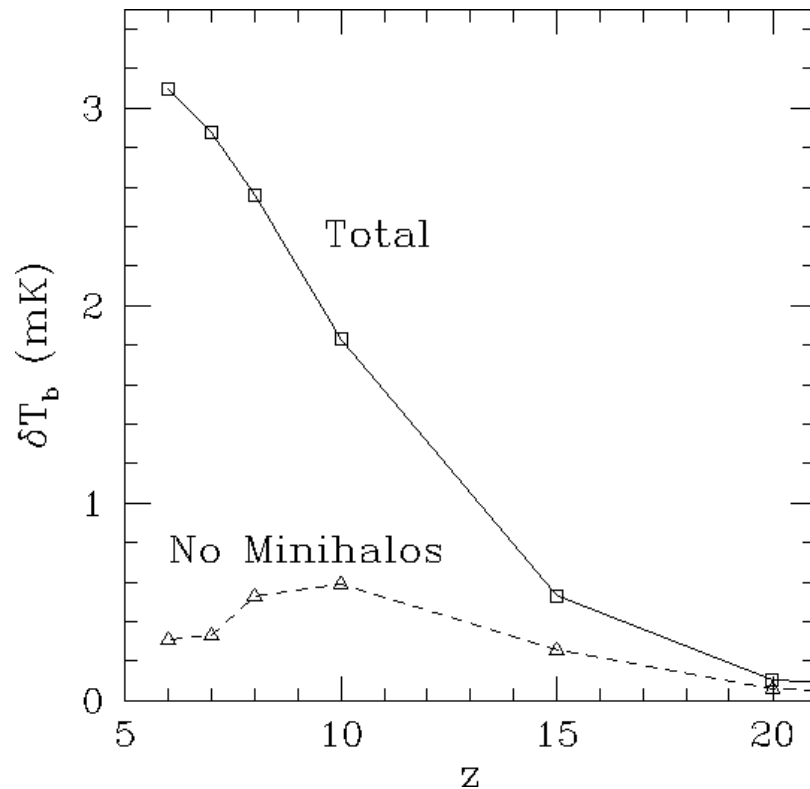
- Shock-heated IGM outside of the minihalos may also contribute to the 21-cm background, despite its less effective collisional pumping (Furlanetto and Loeb 2003).
- To quantify this, we simulated the gas and N-body dynamics of cosmic structure formation in Λ CDM before reionization, to compute the spin temperature at each point and map the differential brightness temperature vs. redshift.
- TVD/PM (Ryu et al. code) simulations with 0.7 Mpc comoving box size used 512^3 cells and 256^3 particles.

TOTAL Z=8



LOG 10 [DIFFERENTIAL BRIGHTNESS TEMPERATURE] (mK)

- Mean brightness temperature is dominated by the minihalos for $z < 15$.
- At $z > 15$, the two contributions, minihalos and shocked gas outside minihalos, become comparable.



Summary

- Standard CDM model of hierarchical structure formation predicts that significant small-scale structure, and in particular large number of minihalos have formed at high- z .
- Early on both minihalos and ionizing sources are very strongly biased. Reionization proceeds in complicated fashion, following neither “dense regions first”, nor “voids first” scenarios.
- Minihalos are self-shielded and trap the global I-fronts during reionization. We performed the first realistic simulations of this process, obtaining that minihalos consume significantly more ionizing photons than the minimum of one per atom, but much less than optically-thin approximations would predict.
- These small-scale structures, both self-shielded minihalos and clumpy IGM, can have significant effect on the progress and duration of reionization, slowing it down and extending it in time, helping to reconcile the WMAP and SDSS QSO constraints on reionization epoch.
- All minihalos at high- z are neutral and sufficiently hot to emit strongly at 21-cm hydrogen line without need of additional heating or Ly- α pumping, allowing direct observations of the Dark Ages, as well as following the progress of reionization.
- Minihalos can also be seen in absorption as individual lines, or as “21-cm GP effect”.
- Sampling this emission and absorption with the existing and future radio telescopes is a great challenge, but would give us unique opportunity to sample early nonlinear structure formation and can provide the only available constraints on density power spectrum $P(k)$ at very small scales with k up to few thousand.
- Finally, we have developed a new fast, precise and efficient method for radiative transfer. Still work in progress, but we hope that new and exciting results would follow soon!